JAERI-M
9496

PIPE RUPTURE TEST RESULTS; 4 INCH PIPE WHIP TESTS UNDER BWR OPERATIONAL CONDITION-CLEARANCE PARAMETER EXPERIMENTS (RUN 5405, 5406, 5407)

May 1981

Syuzo UEDA, Toshikuni ISOZAKI, Noriyuki MIYAZAKI
Ryoichi KURIHARA, Rokuro KATO, Kazuo SAITO*
and Shohachiro MIYAZONO

日本原子力研究所
Japan Atomic Energy Research Institute

この報告書は，日本原子力研究所がJAERI-Mレポートとして，不定期に刊行している研究報告書です．入手，複製などのお問合わせは，日本原子力研究所技術情報部（茨城県那珂郡東海村）あて，お申しこしください．

JAERI-M reports, issued irregularly, describe the results of research works carried out in JAERI. Inquiries about the availability of reports and their reproduction should be addressed to Division of Technical Information, Japan Atomic Energy Research Institute, Tokai-mura, Naka-gun, Ibaraki-ken, Japan.

JAERI-M 9496

Pipe Rupture Test Results; 4 inch Pipe Whip Tests under BWR Operational Condition - Clearance Parameter Experiments (Run 5405, 5406, 5407)

Syuzo UEDA, Toshikuni ISOZAKI, Noriyuki MIYAZAKI, Ryoichi KURIHARA
Rokuro KATO, Kazuo SAITO* and Shohachiro MIYAZONO

Division of Reactor Safety, Tokai Research Establishment, JAERI

(Received April 27, 1981)

The purpose of pipe rupture studies in JAERI is to perform the model tests on pipe whip, restraint behavior, jet impingement and jet thrust force, and to establish the computational method for analyzing these phenomena. This report describes the experimental results of pipe whip on the pipe specimens of 4 inch in diameter under BWR condition on which the pressure is 6.77 MPa and the temperature is 285 °C.

The pipe specimens were 114.3 mm (4 inch) in diameter and 8.6 mm in thickness and 4500 mm in length. Four pipe whip restraints used in the tests were the U-bar type of 8 mm in diameter and fabricated from type 304 stainless steel. The experimental parameter was the clearance (30, 50 and 100 mm). The dynamic strain behavior of the pipe specimen and the restraints was investigated by strain gages and their residual deformation was obtained by measuring marking points provided on their surface. The Pressure-time history in the pipe specimens was also obtained by pressure gages.

The maximum pipe strain is caused near the restraints and increases with increase of the clearance, The experimental results of pipe whip tests indicate the effectiveness of pipe whip restraints. The ratio of absorbed strain energy of the pipe specimen to that of the restraints is nearly constant for different clearances at the overhang length of 400 mm.

Keywords; Pipe Whip, Restraint, Dynamic Strain, Absorbed Energy, Thrust Force, Plastic Hinge, Collision, BWR Type Reactors, Pipe Rupture Test

---

This work was performed under the contract between the Science and Technology Agency of Japan and JAERI to demonstrate the safety for pipe rupture of the primary coolant circuits in nuclear power plants.

* On leave from Ishikawajima Harima Heavy Industries Co. Ltd.

配管破断試験結果；4インチ口径BWRパイプホイップ —クリアランスパラメータ実験

日本原子力研究所東海研究所安全工学部
植田脩三・磯崎敏邦・宮崎則幸・栗原良一
斎藤和男*・宮園昭八郎

（1981年4月27日受理）

本報告は，BWR型原子炉の運転状態において4インチ口径配管が瞬時破断をしたと仮定した時に生じる配管のパイプホイップ運動とそれを抑止するレストレントの挙動に関する実験結果をまとめたものである。本報告に述べる3回の実験は，レストレント設置位置を一定とし，配管とのクリアランスを30，50，100 mmと3種類かえて行った。

試験体に貼付したひずみゲージ，圧力計による電気計測，試験体の残留変形測定，高速度カメラ撮影結果から瞬時破断した場合の配管とレストレントの運動のメカニズムが推察できた。本実験では，レストレントは有効に働いた。配管の歪分布からレストレントとの衝突により，レストレント近傍に弱いヒンジのできることがわかった。また，配管とレストレントの残留歪から吸収エネルギーが評価された。

この報告書は，電源開発促進対策特別会計施行令に基づき，科学技術庁から日本原子力研究所への委託研究，昭和54年度「配管信頼性実証試験の内4B，BWRパイプホイップ試験の結果をまとめたものである。

*）外来研究員；石川島播磨重工業（株）

Contents

目　　次

List of Tables

List of Figures

1. Introduction

Pipe rupture study are being performed in Material Strength and Structure Laboratory, JAERI as one of researches concerning the demonstration test of pipe reliability for a light water reactor. The purpose of the pipe rupture study is to perform model tests using 4, 6 and 8 inch test pipes and to establish the computational method for the jet impingement and pipe whip phenomena which are assumed to be occured in postulated loss-of-coolant accidents of LWR nuclear power plants.

This report describes results of three pipe whip tests of 4 inch test pipe, which were performed in the period of November and December in 1979. The clearance of 30, 50 and 100 mm was taken as the experimental parameter, which is one of the basic parameters[1].

The purposes of these tests are as follows.

1) To investigate the strain distribution of the test pipe and the relationship between the maximum pipe strain and the experimental parameter.
2) To investigate the strain distribution of the restraint and the relationship between the maximum restraint strain and the experimental parameter.
3) To obtain the pressure time history in the test pipe and the pressure vessel.

2. Testing Procedure

2.1 Testing System

The schematic of the pipe whip test is shown in Fig.2.1. An end of an auxiliary connecting pipe was attached to the nozzle of the pressure vessel which was 4 m^3 in volume. There was the attachment for measurement of pipe reaction forces due to the pressure wave in this auxiliary pipe. To the another tip of the connecting pipe, the test pipe was connected. The test pipe was fixed by the pipe support so that the length of test section was 3000 mm.

Four pipe whip restraints were set on a restraint support at the distance of 400 mm from the tip of test pipe, that is to say, the overhang length of this experimental series was 400 mm. Hot water was circulated through the warming-up line which was attached to the elbow of the test pipe in order to keep the system temperature uniform. A flexible tube was used as a part of warming-up line to reduce its resistance against the pipe whip motion. A welded type of the rupture disk was mounted at the tip of the test pipe. Instantaneous pipe rupture was simulated by breaking this rupture disk by an electric arc method. Detail of test equipment is described in reference (2).

2.2 Test Pipe and Pipe Whip Restraints

The test pipe is 4 inch in diameter, 4500 mm in length and 8.6 mm in thickness. Its material is Type 304 stainless steel. The chemical composition and mechanical properties of the test pipe are shown in Table 2.1.

Six nozzles for pressure gages and thermocouples are attached to the

test pipe at the locations as shown in Fig.2.1. The welded type of the rupture disk was butt-welded at the tip of the test pipe. This assembly of the rupture disk was developed especially for pipe whip tests and has a configuration shown in Fig.2.2. This assembly was made by placing a rupture disk between two segments of pipe and sealing them by welding. So the weight of this assembly is nearly equal to that of the ordinary pipe.

The configuration of pipe whip restraint is shown in Fig.2.3. This is called U-type restraint. The clearance is determined from the thickness of insulation and thermal expansion of pipes in nuclear power plant design[3]. The resistance of restraints against design load is adjusted by varying the number of them. The U-bar is made from type 304 stainless steel whose chemical compositions and mechanical properties are shown in Table 2.1. Clevis is screwed to the end of U-bar and used for fine adjustment of the clearance. Restraints are pinned to the bracket which is set on the restraint support. The number of restraints was four in this experiment. The bearing plate of carbon steel was attached to the inner side of the circular part of U-bar. The purpose of this plate was to wrap around the test pipe to minimize the pipe rebound.

Overall view of test assembly of Run 5405 is shown in Photo 1.

2.3 Test Conditions

Test conditions for three experiments are summarized in Table 2.2. The test pressure and test temperature decreased to the extent of $1 \sim 2$ kg/cm^2 and $0.3 \sim 2.4$ degree in centigrade respectively from the nominal test pressure, 69 kg/cm^2, and test temperature, 284.5 °C. As test pipe had a tendancy to hang down from the initial setting point due to the weight of water after pouring water into the pressure vessel, a stopper was provided

to keep the clearance constant during the test.

2.4 Measuring Items and Method

Following three measuring items are performed.

1) Electrical measurement
2) Mechanical Measurement
3) High speed camera photography

(1) Electrical measurement

Measuring items for each test are summarized in Table 2.3. Locations of strain gages from XU109 to XU120 on the pipe are shown in Fig.2.1. Strain gages were high temperature strain gages and mounted on the surface of the test pipe by welding.

Locations of strain gages from XU121 to XU160 on the restraints are shown in Fig.2.4. These strain gages were those used at room temperature. Restraints are named R1, R2, R3, and R4 respectively in order from the side of the pipe end.

Strain gages in the part of clevis were those used for small strain and strain gages in other part were those used for large strain. They were covered with coating for protecting them from hot steam. All strain gages were single.

Pressure and temperature were measured in both the pressure vessel and the test pipe. Pressure-time histories of the test pipe were measured by pressure transducers PU110, PU111 and PU112. Two types of pressure transducers were used, that is to say, the water-cooling type and the high temperature type. Thermocouples TU130, TU131 and TU132 were used for measurement of fluid temperature and the response time of them was about 2 seconds. Thermocouple TU133 was mounted on the surface of the test pipe and

temperature variation of the test pipe during the blowdown was monitored. Load cell WU101 was used for the measurement of the mass flow rate. Water level meter WU115 was a pressure differential type and used for the measurement of the mass flow rate. Load cell WU111 was placed behind the elbow of the auxiliary connecting pipe to measure the thrust load due to the pressure wave propagation. This load cell was contacted closely with the test pipe by U-bolt restraint. Displacement meters XU-200 and XU-201 were eddy current type and placed at the location of 700 mm from the tip of the test pipe. Accerelometers XU300, XU301 and XU302 were placed at the locations shown in Fig.2.1.

The amplified outputs were recorded in the analog data recorder. Response frequency of the total data aquisition system was over 20 kHz. The initial point of recording was the time when the electric current initiated to flow in the arc electrode. The arc current started just after the state of the data recorder and high speed camera attain the steady state. Also some of pressures and temperatures in the pressure vessel were recorded in the disk of the computer in on-line mode.

On-line recording was started manually ten seconds before breaking of a rupture disk. The sampling time of on-line mode was 10 msec.

(2) Deformation measurement by mechanical tool

Measurements were done before and after tests for the distance between marks. Measured items were as follows.

1. Residual strains of pipes; Axial distances between markings of 100 mm interval on the upper and lower surfaces of test pipes were measured. Markings were made from the tip of the test pipe to the location of 1000 mm.
2. Residual displacement of pipes; The hight of marking points from the

base level was measured by a transit before and after tests.

3. The variation of the outer diameters of test pipes
   (a) Run 5406, 5407; Measurement was done at the circumferential intervals of 30 degrees at the location of 370 mm from the tip of the test pipe.
   (b) Run 5407; Measurement of the horizontal and vertical diameters was done at the intervals of 50 or 100 mm from the pipe tip to the location of 1300 mm.
4. Residual strains of restraints; Measurement of the length between each marking was done.
5. The height of restraints; Measurement of the height between the centre of the pin and the apex of restraints was done. Nominal design values were taken as values before tests.

Measuring tools were slide calipers, micrometers or height gages.

(3) High speed camera photography

Two high speed cameras were used. One was used for the overall view and the other was used for the view near restraints. A steam screen was used for protect objects from steam. Photographing conditions are shown in Table 2.4.

3. Test Results

3.1 Electrical Measurement

(a) Pressure in the pressure vessel

Pressure-time histories are simular for all the experiments because test pressure, temperature and the configuration of the test pipe are nearly same. So representative curves are discussed in this paragraph. Pressure-time histories in the pressure vessel (PU101, 105) are shown in Fig.3.1 and 3.2. Pressure in the vessel does not almost change in the range of 0.1 sec after the initiation of the blowdown. Pressure drops about 3 kg/cm^2 in the 0.5 sec and thereafter reduces slowly. The nee where the blowdown change from a hot water one into a steam one appears at 18 second after the initiation of the blowdown. Thereafter pressure drops rapidly and the total blowdown time is over 100 sec.

(b) Pressure in the test pipe

The representative curves of the pipe pressures, PU110, PU111 and PU112 are shown in Figs.3.3, 3.4, and 3.5. Pressures drop in the stepwise manner just after the initiation of the blowdown and thereafter do not almost change in the range of 1.0 second. Pipe pressures reduce to the 40 kg/cm^2 in 1.0 second. After that time pressures reduce slowly and also the knee appears at 18 second as shown in Fig.3.6.

(c) The fluid temperature in the vessel and pipe

The response time of thermocouples is 2 second, so meaning results could not be obtained within this duration. From 2 second to 60 second temperatures followed a saturation curve. After 60 second temperature rised over the saturation point because of heating by vessel wall.

(d) Output of load cell WU111

As stated later, the output of load cell means the thrust by the pressure difference due to the wave propagation. This thrust disappears after 0.3 second as shown in Fig.3.7.

(e) Water level in the pressure vessel, WU115

The representative output of water level meter is shown in Fig.3.8. The water level reduces linearly during 2 and 15 second.

(f) Strain

The interpritation of the dynamic strains of the pipe and restraint are discussed in detail in the paragraph 4.1. Generally speaking, Transient behavior of strains terminated within 0.1 sec after the initiation of the blowdown in these experiments. This fact indicates that the pipe whip phenomena is a problem in the initial stage of the LOCA phenomenon.

(g) Acceleration and displacement

At present useful results could not be obtained.

3.2 Results of Residual Deformation Measurement

1. Residual strains of the test pipe

Results are summarized in Table 3.1 and the distribution of residual strains are shown in Fig.3.9. Peak values occur in the vicinity of the restraint's position but not just below the restraints.

2. Residual deformation of the test pipe

Results are summarized in Table 3.2, and plotted in Fig.3.10.

3. Measurement of outerdiameter of the test pipe

Results in Run 5407 are shown in Fig.3.11. The test pipe expands in

the horizontal direction and contracts in the vertical direction.

5. Deformation of the restraint

Front view of restraints after tests are shown in Fig.3.12. Appearances of the test section including restraints after tests are shown in Photo 2. It can be seen that the restraint deformed from initial shape and stretched like stringents. It can also be seen that the bearing plates wrap around the test pipe and comform to the bending pipe surface.

3.3 Observation of Pipe Whip Phenomenon by High Speed Camera

Photographs taken by high speed cameras are shown in Photo 3. Overall views and local views near restraints are included in this photograph. In Run 5405, frames start at 1.7 msec after the initiation of blowdown. They start at 0.6 msec in Run 5406 and at 52.5 msec in Run 5507. Frame intervals are described in this photograph.

In all experiments the bearing plate rotate after collision and this fact means that the bearing plate conform to the bending pipe surface. In Run 5407 restraints slided in the aixal direction of the test pipe at 59 milliseconds after the initiation of the blowdown although this phenomenon was not seen in Run 5405 and Run 5406. This sliding seems to increase the upward movement of the test pipe. Displacement-time history analyzed from films, at the distance of 400 mm from the tip of the test pipe is shown in Fig.3.13. Data of three experiments are nearly plotted on the same curve. The impact velocities of the test pipes and restraints analyzed from this curve are about 5 m/sec in Run 5405 and Run 5406, and 10 m/sec in Run 5407 respectively.

4. Consideration

4.1 Time Sequence of Events in Pipe Whip Phenomenon

Pressure-time histories in the pressure vessel and the test pipe, PU103, PU111, strain-time history of the pipe, XU110, strain-time history of the restraint, XU125 are shown in Fig.4.1. The abscissa is in the range of 0 - 1.0 second. Pressure drops abruptly in stepwise manner at the initiation of the blowdown and recover to some extent and then decrease slowly. However both strain of the test pipe and that of the restraint attain the steady state within 100 milliseconds in the initial stage of this blowdown process.

Time sequences of various events are analyzed from electrical measurement and shown in Fig.4.2. The starting time of output of the acceleration meter at the tip of the test pipe is taken as the initiation of the blowdown. The variation of strains of the test pipe and pressure in the test pipe PU110 started at the same time. The difference between the impact time between the test pipe and each restraint was within 1 msec. This time is longer with increase of the clearance.

4.2 Deformation of Test Pipe

(1) Residual deformation

Appearances of the test section after the experiments are shown in Photo 2 . It can be said from Fig.3.9 that the distribution of residual strain has the peak value near the restraints. The peak is located at a distance of 50 ~ 100 mm backward from the restraints in Run 5405, 5406 and at a distance of 100 ~ 200 mm backward from the restraints in Run 5407. The value of the peak strain in Run 5406 is smaller than those in other experiments. This fact could not be hardly explained at present. However the displacement of the pipe and strains of restraints is also in the same trend.

The residual pipe strain reduces to the zero value at the distance of 200 mm from the peak point in the pipe tip direction. The residual strain reduces to the zero value at the distance of 200 mm from the peak location and increase again and make the second peak which is lower than the first one in the direction of the fixed end. Therefore the peak region is confined within the distance of several diameters of the test pipe and this fact means that the insufficient plastic hinge is formed at this location.

The simular shape of the distribution was obtained in the measurement of the outer diameter in the experiment Run 5407 (Fig.3.11). The local buckling was not observed on the compressive side of the test pipe at the location of the restraints.

(2) Dynamic strain behavior

The dynamic behaviors of the strain of the test pipe can be classified into two groups, that is to say, strains of the test pipe near the restraints and strains at other positions. Representative strain-time histories are shown in Fig.4.3. Strains near the restraints increases gradually after the initiation of the blowdown until the test pipe impacts the restraints. After impacting, strains increase rapidly, go into the plastic region and attain the steady state.

Strains, for example, XU117, XU118 between the fixed end and the restraint at first increase monotonically before the impact and reduce backward enforcedly after the impact between the test pipe and restraints and finally vibrate. This viabration mode is bending because of the symmetry of strain values of the upper and lower surface. The time of the first peak in the strain-time history concide with the time of the impact. The period of vibration is 25 msec and slightly bigger than the calculated period by FEM method, which is described in the appendix. The trend that

strains go to the opposite direction after impact is not so clear at positions near the fixed end. (XU119, 120). In the experiment Run 5407, these vibrations damped rapidly because of the large plastic strain.

4.3 Deformation of Restraints

(1) Dynamic behavior

Outputs of strain gages on the straight part of the restraints are shown in Fig.4.4. One pair of the inner strain and outer one are superposed in this figure. The dotted line is the mean value of one pair of outputs. It can be saids from outputs of all strain gages that in several millisecond after collision, strain gage vibrate in bending mode without axial extension. This means that it takes several milliseconds from the impact time to the time when restraints are effective for stopping the motion of the test pipe. The dynamic strain behaviors of restraints seem to be classified into two groups.

The first one is the output of restraint R1, in each experiment. The strain of this group behaves in such like that it vibrate in short duration just after the collision, then increase rapidly to the first peak, thereafter increase gradually to the final steady state. The strain rate in the rapidly increasing duration attained 10/sec in Run 5407. Output of other strain gages belongs to the second group. In this group, the first peak strain or the strain in the transient state is larger than that in the steady state. Some of strains are in the plastic region, for example, those of restraint R2 in each experiment.

Other outputs in this group are in the region of elastic strain. The strain has the small peak just after the collision and then vibrate in bending mode. Periods of this vibration are 15 msec and 8 msec. The strain

behavior near the clip in the circular part of the restraints are shown in Fig.4.5. Until the pipe reach the effective clearance after the collision, strains at this location rapidly go into the minus strain region.

This is because the bearing plate pull U-bar into the inside direction when it wraps around the test pipe and the U-bar bends such as reducing its curvature. After this phenomena, strains in restraint R1 in Run 5405, 5407 go to the plus strain because of the substantial axial extension due to the further pipe motion.

(2) Deformation

In Figs.4.6 through 4.8 the residual strain distribution of each run is shown. The distribution is uniform in the straight part of the restraint but is not uniform in the circular part of the restraint.

Strain near the apex of the restraint is several times larger than that in the straight part of the restraint. As the residual strains were measured on the outer side of the restraints, this large strain may include the bending strain component. However the average extensional strain in the circular part was not so differ with that in the straight part from results of another experiment which will be published in the future. Therefore strains in the straight part of restraints were chosen as the representative one and they were compared concerning 4 restraints in each experiment.

The first peak strains and steady state ones in each experiment are illustrated in Figs.4.9. The value of strain of restraints R1, R2, R3 and R4 become smaller in their order. Also the first peak strain of the restraint R1 is smaller than that in the steady state in all experiments. This fact means that four restraints don't bear the blowdown force equally during the blowdown and also the ratio at which each restraint bear the

blowdown force varies with the time. Strains of restraint R1 in Run 5406 are the smallest although the clearance is intermediate.

The reason has not been yet clarified. The maximum strain of the restraint is 2.4% in the straight part and 5.8% in the curcular part in Run 5407. There is an important difference of deformations of the restraints between Run 5405, 5406 and 5407 as already described in paragraph 3.3.

Restraints inclined due to the folding near the welded joint between U-bar and part of screw in Run 5407 although this phenomenon was not observed in Run 5405 and 5406. The slope is twelve degrees and the apex of the restraint transfered about 100 mm in the backward. This is because the pipe collides obliquely with the restraints with increase of the clearance.

4.4 Relation between Dynamic Behaviors of Test Pipe and Those of Restraints

In Fig.4.10 the representative outputs of strain gages in each run are shown for the discussion of the mode of the pipe whip motion. From this figure it can be said that there are four modes of motion described as follows.

Stage I: the movement of the test pipe from the initial position to the effective clearance after the collision between the test pipe and the restraints.

Stage II: the pipe movement till the end of the substantial extensional deformation of the restraints.

Stage III: the pipe movement till the steady state of the strain of the test pipe.

Stage IV: the additional movement of the test pipe and restraints due to the inclination of the restraints.

In the stage I, the pipe rotates on its fixed end and collide with the restraint and move together to the effective clearance. Restraints only

wrap around the test pipe and don't prevent the pipe movement during this stage. In the stage II the restraints restrict the test pipe motion and also restraints are subjected to the extensional load in the same time. The rotation of the pipe on its fixed end is over in this stage and a preliminary hinge is formed around the restraints. The pipe rotates on this hinge. In the stage III, mainly, the pipe rotates on the formed hinge. In case of Run 5406 this mode cannot be seen. There is stage IV in Run 5407. In this stage restraints incline, slides backward and the pipe rotates again on its fixed end.

The duration from the initiation of the blowdown to the end of the motion of the pipe and restraints is about 20 msec in Run 5405, 5406 and about 60 msec in Run 5407 respectively.

4.5 Reaction Force of Restraint Support

In this paragraph the reaction force of the restraint support is coarsely evaluated from total outputs of strain gages at the straight parts of the restraints. The effect of unloading by vibration and the effect of strain rate on the stress-strain law were neglected in this evaluation. The strain values are taken from Table 3.8. The stress-strain curve was obtained from the tensile test. Calculated reaction forces for each restraint are summarized in Table 4.1. The total reaction force of restraints is shown in Fig.4.12. The maximum value is 16 ton in Run 5407.

4.6 Absorbed Strain Energy of Test Pipe and Restraints

Absorbed strain energies of the pipe and restraints are evaluated in this paragraph. The evaluation was done under the following conditions.

1. Strains of the straight parts of restraints in Table 3.6 are used for the energy evaluation. The vibration energy is neglected.

2. Only U-bar rod is taken into account for the energy evaluation. The bending deformation of U-bar is neglected.
3. The strain distribution of the pipe is approximated by multi-linear curve. The strain values are taken from Table 3.2.
4. The stress-strain law is $\sigma = k\ \varepsilon^n$ as shown in Fig.4.11. The effect of the strain rate is neglected.

As the amplitude of vibration in the strain-time history at the important locations is small, assumptions 1, 4 is relevant. Equations for the absorbed energy calculation are as follows.

(1) Restraints

$$E_R = \int_o^{\ell} A\,ds \int_o^{\varepsilon_o} \sigma\,d\varepsilon$$

$$= \frac{K}{n+1}\,\varepsilon_o^{n+1} \times V$$

where

E_R : Absorbed strain energy of restraint

ε_o : Restraint strain

V : Volume of U-rod

K,n : Material constant

A : Section area of U-bar

(2) Test pipe

Strain distribution in the pipe section is assumed to be linear.

$$\varepsilon(x,y) = \frac{\varepsilon_o(x)}{R_o} \cdot y$$

x : Coordinate in axial direction (x = 0, at fixed end)

y : Coordinate in vertical direction (y = 0, at neutral axis)

$\varepsilon_o(x)$: Maximum surface strain at location x

$$\sigma(x,y) = K\,\varepsilon(x,y)^n$$

$$E_p = \int_o^L dx \left[2\int_o^{R_o} 2\sqrt{R_o^2 - y^2}\, dy \int_o^{\varepsilon} \sigma(x,y)\, d\varepsilon - 2\int_o^{R_i} 2\sqrt{R_i^2 - y^2}\, dy \int_o^{\varepsilon} \sigma(x,y)\, d\varepsilon \right]$$

$$= \frac{4K}{n+1}\frac{1}{R_o^{n+1}} \int_o^L \varepsilon_o(x)^{n+1} dx \left[\int_o^{R_o} y^{n+1} \sqrt{R_o^2 - y^2}\, dy - \int_o^{R_i} y^{n+1} \sqrt{R_i^2 - y^2}\, dy \right]$$

$$= \frac{4K\, I_n}{(n+1)(n+3)R_o^{n+1}} (R_o^{n+3} - R_i^{n+3}) \int_o^L \varepsilon_o(x)^{n+1} dx$$

where

R_o : Outer diameter of test pipe

R_i : Inner diameter of test pipe

L : Pipe length

$$I_n = \int_o^{\pi/2} \sin\theta^{n+1}\, d\theta \doteqdot 1 - 0.291\, n + 0.076\, n^2 \quad (5)$$

E_p : Absorbed strain energy of test pipe

Calculated results are summarized in Table 4.2 and illustrated in Fig.4.13. The external work by the blowdown force is also shown in this table although the blowdown force is assumed to be constant. The absorbed strain energy of the test pipe is several times larger than that of restraints as shown in this figure. The ratio of absorbed strain energy of the restraints to that

of the pipe is 19% in Run 5405, 5406 and 14% in Run 5407.

The ratio of absorbed energy is clearly insensitive to the clearance. These facts means that the role of restraints is not rather to absorb the pipe whip energy but to resist against the motion of the test pipe and to convert the kinetic energy of the test pipe to the strain energy of the test pipe.

4.7 Pressure Depressurization in Test Pipe just after Initiation or Blowdown

Pressure in the test pipe is depressed in stepwise way just after the rupture of the rupture disk as shown in the Fig.4.14 of pressure-time history in the range of 0 - 0.1 sec. The pressure measurement in long term was not succeeded in these experiments. However the initial depressurization quantity is reproducible. These quantities are shown in Fig.4.15. The quantity of depressurization is about 30 kg/cm^2 at the tip of the pipe and reduce with increase of the distance from the exit. The time of the initiation of depressurization become later with increase of the distance from the exit. Velocity of the pressure wave calculated from the time difference of the initiation of depressurization at different locations is 940 m/sec.

4.8 Explanation on Measurement of Pipe Reaction Force (WU111)

In this paragraph equations for calculating reaction forces are described following the feferences[6][7]. A pipe segment which include two elbows is illustrated in Fig.4.16. At first general equations are deduced. The fluid forces which may act on the pipe surfaces are expressed by the next equation.

$$\bar{F} = \iint_{S_W} p\bar{n}dS_W + \iint_{S_W} \bar{\tau}dS_W \tag{1}$$

The momentum equation which the fluid obey is

$$\Sigma \bar{F} = \frac{\partial}{\partial t} \iiint_V \frac{\bar{u}}{g_c} + \iint_{S_1} \frac{\bar{u}}{g_c} (\rho\bar{u} \cdot \bar{n})_1 \, dS_1 + \iint_{S_2} \frac{\bar{u}_2}{g_c} (\rho\bar{u} \cdot \bar{n})_2 \, dS_2 \tag{2}$$

The forces acting on the fluid are

$$\bar{F} = - \iint_{S_W} p\bar{n}dS_W - \iint_{S_W} \bar{\tau}dS_W - \iint_S p_1 n_1 dS_1 - \iint_{S_2} p_2 \bar{n}_2 dS_2 - \iiint_V \frac{g_c \bar{K}}{g_c} dV \tag{3}$$

after equating eqs.(2), (3), the common terms of eq.(1) are identified

$$\bar{F} = - \{ \frac{\partial}{\partial t} \iiint_V \rho \frac{\bar{u}}{g_c} dV + \iint_{S_1} [p_1 \bar{n}_1 + \frac{\bar{u}_1}{g_c} (\rho\bar{u} \cdot \bar{n})_1] \, dS_1 + \iint_{S_2} [p_2 \bar{n}_2 + \frac{\bar{u}_2}{g_c} (\rho\bar{u} \cdot \bar{n})_2] \, dS_2 + \iiint_V \frac{\rho g_a}{g_c} \bar{k} \, dV \} \tag{4}$$

Forces acting on the pipe consist of acceleration term, pressure term and momentum flux term. Momentum balance of the axial direction of the pipe which has two elbows on both end as illustrated in Fig.4.16

$$F_1 - F_S - F_2 = [F_{11} - (p_1 - p_\infty)A_1 - \frac{\dot{m}_1 u_1}{g_c}] \cos\alpha_1 - [F_{22} - (p_2 - p_\infty)A_2 - \frac{\dot{m}_2 u_2}{g_c}] \cos\alpha_2 + \frac{1}{g_c} \frac{\partial}{\partial t} \int_o^{L_i} \rho A u dZ \tag{5}$$

When the control volume is divided by dotted line as shown in Fig.4.16, Forces vertical to the axis do not occur due to pressure and flow. Momentum balances of two separate volumes are

$$[F_{11} - (p_1 - p_\infty)A_1 - \frac{\dot{m}_1 u_1}{g_c}] \sin \alpha_1 = 0$$

$$[F_{22} - (p_2 - p_\infty)A_2 - \frac{\dot{m}_2 u_2}{g_c}] \sin \alpha_2 = 0$$

$\text{Sin}\alpha_1$, $\text{sin}\alpha_2$ are not zero in case of 90 degree elbow. Therefore,

$$F_{11} = (p_1 - p_\infty)A_1 + \frac{\dot{m}_1 u_1}{g_c}$$

$$F_{22} = (p_2 - p_\infty)A_2 + \frac{\dot{m}_2 u_2}{g_c}$$

Also, in case of 90 degree elbow, Axial force $(F_1 - F_S - F_2)$ only contain acceleration term. This means that the pipe thrust forces arising at pipe exit do not propagate upward except acceleration term when the pipe is bent in 90 degree. As acceleration term disappear in steady state, axial force is zero at steady state. Load measurement by load cell WU111 is just the case explained above. As shown in Fig.3.7 with regard to load-time history in the range of 0 to 1.0 second, actually load due to pressure wave disappear within 0.3 seconds after the initiation of the blowdown.

4.9 Discharging Mass Flow Rate in the Steady State

Discharging mass flow rate is nearly constant in this system from 2 seconds to 15 seconds after the initiation of the blowdown. The mass flow

rate in the steady state was calculated from the output of the level meter in the pressure vessel by the next equation.

$$G = \rho\pi R^2 \cdot \frac{dL}{dt}$$

where $\rho = 761.6\ kg/m^3$

L = Fictious water level

Calculated G values are 1.44, 1.41, 1.45 $kg/m^2 \cdot sec$, in order of Run 5405, 5406 and 5407 respectively.

5. Concluding Remarks

1) The mode of pipe whip motion analyzed from experimental results is as follows. After the rupture disk is broken by the electric arc method, the high temperature water initiates to blow, the test pipe initiates to rotate on its fixed end and is accerelated. The test pipe collides with restraints after it is accelerated to the velocity of 5 m/sec (Run 5404, 5406) or 10 m/sec (Run 5407). The restraints do not resist against the pipe whip motion until the test pipe reaches the effective clearance. Restraints absorb the kinetic energy of the pipe by their plastic deformation and also convert the kinetic energy of the test pipe to the strain energy of the pipe by resisting against pipe motion. The duration of pipe whip phenomena is about 20 msec in Run 5405, 5406 and 60 msec in Run 5407 respectively.

2) With regard to the strain distribution of the test pipe, the peak strain occurs near the restraints. This fact means that the insufficient plastic hinge is caused at the time of collision between the test pipe and restraints in Run 5405, 5407. The maximum axial pipe strain is 4.0 percent in Run 5407.

3) The assembly of four restraints is used in these tests. Restraint No.1 on the side of discharging exit works best for limitation of the pipe whip motion. The bearing plate wrapped around the test pipe sufficiently. However this bearing plate is clipped at the restraint and therefore the strain distribution of restraints is complicated. However the strain in the straight part of restraint may be the representative one which indicate the degree of deformation. Experimental certification will be performed in next experiments.

4) The absorbed energy of restraints is much less than that of the test

pipe. This fact means that the purpose of U-bar restraint is mainly to limit the pipe whip motion by its resistance as far as these experiments are concerned.

5) The mass flow rate in the steady state is 1.44, 1.41 and 1.45 $kg/cm^2 \cdot sec$ in Run 5405, 5406 and 5407 respectively.

Acknowledgement

This work was performed under the contract between the Science and Technology Agency of Japan and JAERI to demonstrate the safety for pipe rupture of the primary coolant circuits in nuclear power plants.

The authors would like to appreciate the members of Committee on the Assessment of Safety Research for Nuclear Reactor Structural Components in JAERI (Chairman: Prof.Y.Ando, University of Tokyo) for their useful comments. Also the authors would like to appreciate Dr.M.Nozawa, Head of division of Reactor Safety, Reactor Safety Research Center, JAERI for his great support.

pipe. This fact means that the purpose of U-bar restraint is mainly to limit the pipe whip motion by its resistance as far as these experiments are concerned.

5) The mass flow rate in the steady state is 1.44, 1.41 and 1.45 $kg/cm^2 \cdot sec$ in Run 5405, 5406 and 5407 respectively.

Acknowledgement

This work was performed under the contract between the Science and Technology Agency of Japan and JAERI to demonstrate the safety for pipe rupture of the primary coolant circuits in nuclear power plants.

The authors would like to appreciate the members of Committee on the Assessment of Safety Research for Nuclear Reactor Structural Components in JAERI (Chairman: Prof.Y.Ando, University of Tokyo) for their useful comments. Also the authors would like to appreciate Dr.M.Nozawa, Head of division of Reactor Safety, Reactor Safety Research Center, JAERI for his great support.

References

(1) N. Miyazaki, Y. Kannoto and R. Kurihara "The effect of various parameters on pipe whip phenomena" Vol.21 No.6 Journal of JNS 1979.

(2) T. Isozaki et al "Outline of pipe rupture test facilities", Internal Report (1979).

(3) G. Esswein, S. Levy, M. Triplett, G. Chan and N. Varadarajan: "Pipe Whip Dynamics", ASME 1977 PVP-PB-022, Dynamic Analysis of Pressure Vessel and Piping Components.

(4) N. Miyazaki, K. Saito "PRILIMINARY ANALYSIS FOR PIPE WHIP TEST — RUN No.5319", JAERI-M 8487.

(5) T.L. Gerber "Plastic Deformation of Piping Due to Pipe-Whip Loading", ASME Paper, 74-NE-1.

(6) F.J. Moody "Fluid Reaction and Impingement Loads", Nuclear Power Plants, (1973) PP.219 - 262.

(7) Strong, B.R.Jr., Bashiere, R.J. "Pipe Rupture and Steam/Water Hammer Design Loads for Dynamic Analysis of Piping Systems", Nuclear Engineering and Design, Vol.45, (1978), PP.419 - 428.

Appendix: Natural Period of Restraints and Test Pipe

Experiments for getting natural period of the restraint was done and also analytical natural periods of the restraints and the test pipe were calculated by the general purpose finite element code ADINA.

a) Experimental natural periods

Three kinds of restraint were set on the bracket. Strain gages were mounted on the inside and outside of the U-bar. Restraints were hit by a hammer in the transverse and vertical direction and outputs of strain gages were observed by an oscilloscope. Experimental natural periods were ones of the first and second modes and the mode of natural vibration was bending one. Results are shown in table A1. Natural periods of the restraint of the clearance of 100 mm are 108 msec in the first mode and 16 msec in the second mode. Natural periods very slightly with the clearance.

b) Analytical natural periods

Finite element model of the restraint used in calculation and calculated natural modes of vibration are shown in Fig.A1. Calculated natural periods are summarized in table A2. The calculated values are small to the extent of 20% in comparison with experimental ones in the first mode and nearly equal in the second mode.

Finite element model of the test pipe is shown in Fig.A3. Example of calculated modes is also illustrated in this figure. The boundary condition at the restraint is a pin support or a damper support. Calculated conditions and results are shown in Table A3. The long natural period of 103.5 msec appear in case of the damper support but this period was not observed in pipe whip experiments. The first natural period in case of the pin support is 16.5 msec and is nearly equal to the period of 25 msec appeared in pipe whip experiment.

Table 2.3 List of Measuring Items

TAG.NO	LOCATION	SPECIFICATION	MANUFACTURER TYPE	RECORD DEVICE *	**	*** 5	6	7
STRAIN GAGE - PIPE								
XU109 XU110 ↕ XU120	SEE FIG. 2-1	HIGH TEMP. π TYPE HIGH TEMP. SPOT WELDED PLASTIC	ST-LABO SHT10-2 AILTECH SG-125-01F-10		M ↕ M			⊠
STRAIN GAGE - RESTRAINT								
XU121 ↕ 124	RESTRAINT NO.1 (R1)	ELASTIC	KYOWA KFC-2-C1-16		M ↕ M			
125 ↕ XU130	SEE FIG. 2-4	PLASTIC	TOKYO SOKKI YL-5		M L M			
XU131 ↕ 134	RESTRAINT NO.2 (R2)	ELASTIC	KYOWA KFC-2-C1-16		M ↕ M			
135 ↕ XU140	SEE FIG. 2-4	PLASTIC	TOKYO SOKKI YL-5					
XU141 ↕ 144	RESTRAINT NO.3 (R3)	ELASTIC	KYOWA KFC-2-C1-16		M ↕ M			
145 ↕ XU150	SEE FIG. 2-4	PLASTIC	TOKYO SOKKI YL-5					
XU151 ↕ 154	RESTRAINT NO.4 (R4)	ELASTIC	KYOWA KFC-2-C1-16		M ↕ M			

TAG.NO	LOCATION	SPECIFICATION	MANUFACTURER TYPE	RECORD DEVICE		5	6	7
XU155 ↕ XU160	SEE FIG. 2-1	PLASTIC	TOKYO SOKKI YL-5	H ↕ H				
PRESSURE								
PU101	SEE FIG. 2-5	STRAIN GAGE TYPE	BLH GP-H	ON	L			
103				ON	L			
105					L			
110			ST-LABO PHT-100S		H			
111					H	⊠	⊠	
112					H			
112			KYOWA PE-200KJ		H			
113			ST-LABO PHT-5T	ON	L			
114			KYOWA PGM-5KC	ON	L			
115			ST-LABO PHT-5T	ON	M	⊠	⊠	
PU116			KYOWA PGM-5KC	ON	L			
TEMPERATURE								
TU101	SEE FIG. 2-1	C-A SHEATH TYPE	OKAZAKI T-35	ON				
102				ON				
104				ON				
130			SUKEGAWA					
131								
132				ON				
133	NEAR 4B G.L. FLG.			ON				
134	TAGET BOX							
LOAD								
WU101	SEE FIG. 2-1	STRAIN GAGE TYPE	BLH T2G-1	ON	L			
111			KYOWA LC5TFH		L			
DISPLACEMENT								
XU200	SEE PHOTO 2.1	EDDY CURRENT YPPE	SHIN NIPPON SOKKI NP-1000 (503-F)					
201								
ACCELERATION								
XU300	SEE FIG. 2-1	PIEZOELECTRIC TYPE	SHIN NIPPON SOKKI 541-ASH					
301								
302								
WATER LEVEL								
WU115	SEE FIG. 2-1	PRES.DIFF. TYPE	FUJI FEC-3-4-W3-1	ON				
ADDITIONAL STRAIN GAGE								
XU161	U-BOLT SUPPORT	ELASTIC	KYOWA KFC-2-C1-16	ON	L		⊠	⊠
161	U-BOLT		AILTECH SG-125	ON	L		⊠	⊠
162	5406 : R3		KYOWA KFC-2-C1-16	ON	L		⊠	⊠
163	5407 : R1			ON	L		⊠	⊠

* : Blank-Analog Data Recorder (Off-Line), ON-Temporally Digital Memory (On-Line)

** : H - High Freg. Amp. (50KHZ) M - Medium Freg. Amp. (10KHZ)
L - Low Freg. Amp. (2KHZ)

*** : X means that it is not measured in RUN 5405, 5406, 5407, respectively.

Table 2.4 High Speed Camera Conditions

	5405		5406		5407	
VIEW	Whole	Restraint	Whole	Restraint	Whole	Restraint
SPEED (FRAME/SEC.)	4200	5000	5000	5000	4000	5000
LENS	(9.5∿57) 57 m m	75 m m	(9.5∿57) 57 m m	75 m m	6.5 m m	(9.5∿57) 57 m m
DISTANCE	3.1 m	3.2 m	3.1 m	3.2 m	3.1 m	3.3 m
IRIS	F4.0	F4.0	F2.6	F2.6	F2.8	F2.5

Cameras Are HYCAM 41-0004 Typ. with Shutter Constants of 1/2.5 in All Cases.

Sixteen (16) of 1.5 KW Filament Lamp Are Used.

Freq. of Timing Pulse in Film Edge Is 1000 PPS in All Cases.

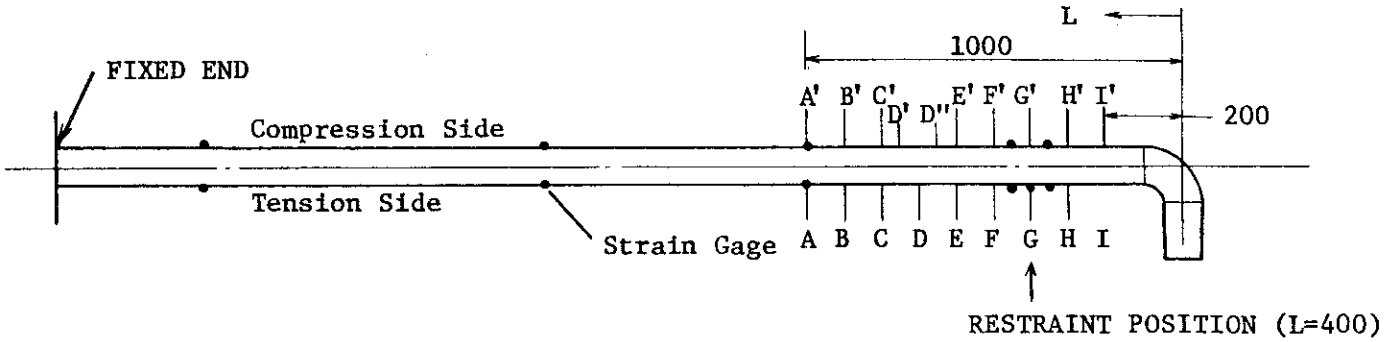

Table 3.1 Residual Strains of Test Pipe (from Dimensional Measurement)

	A-B	B-C	C-D	D-E	E-F	F-G	G-H	H-I		A'-B'	B'-C'	C'-D'	D'-D''	D''-E'	E'-F'	F'-G'	G'-H'	H'-I'
5405																		
B	100.00	100.35	100.00	100.00	100.00	100.00	100.10	100.10		100.00	99.85	49.85	99.40	49.95	100.00	99.80	100.15	100.00
A	100.25	100.60	100.40	100.90	101.45	102.40	101.25	100.15		99.40	99.60	49.60	99.40	49.40	98.65	97.70	98.90	99.95
5406																		
B	100.00	100.15	100.40	99.95	99.90	100.00	99.90	100.00		100.10	100.00	50.00	100.20	49.90	99.80	100.10	99.95	99.90
A	100.50	100.35	100.60	100.15	100.65	100.65	100.40	100.00		99.80	99.70	49.85	99.80	49.60	99.25	99.25	99.50	99.85
5407																		
B	100.00	100.35	100.20	99.80	100.20	99.85	100.10	100.00		100.20	100.10	50.20	100.10	49.80	99.95	100.20	100.00	100.00
A	102.15	102.25	102.10	102.80	104.50	103.85	101.80	100.30		98.45	97.90	49.40	99.55	48.11	95.85	96.45	98.85	100.45

(m/m)

B : Length Before the Tests

A : Length After the Tests

Table 3.2 Residual Strains of Test Pipe (from Strain Gages)

(Micro Strain)

L		250	350 *			450 *		550	650	750	850	950	1000*	1700*	2600*
5405 **	T.Side	500	11500	10900	16400	24000		14500	9000	4000	2500	2500	-	780	60
	C.Side	-500	-12500	-12600		-21000	-17300	-13500	-11000	-5000	-2500	-6000	-	-860	-100
	AVE.	500	11900		16400	20800		14000	10000	4500	2500	4300	-	800	100
5406 **	T.Side	0	5000	5400	6400	6500	6000	7500	2000	2000	2000	5000	2800	900	200
	C.Side	-500	-4500	-4800		-8500	-	-5500	-6000	-3000	-3000	-3000	-4800	-800	-200
	AVE.	250	4900		6400	7000		6500	4000	2500	2500	4000	3800	900	200
5407 **	T.Side	3000	17000	12900	25500	40100	-	42900	30100	19000	18900	21500	-	1300	1100
	C.Side	4500	-11500	-9400		-37400	-	-41000	-33900	-15900	-22000	-17500	-	-2100	-700
	AVE.	3800	12700		25500	38800		42000	32000	17500	20500	19500	-	1700	900

* : Steady State Value of Strain Gage. ** : Averaged Absolute Values of Tension & Compression Side Strains.

Table 3.3 Displacement of Test Pipe

(m/m)

POSITION*	5405	5406	5407
200	63.7	58.6	254.5
600	23.8	30.3	116.0
1000	12.4	20.3	51.5
1400	7.7	8.8	28.5
1800	5.5	4.3	17.5
2200	4.0	0.3	10.5
2600	2.0	-0.7	4.5
FIXED END	0.0	0.0	0.0

* Distance From Pipe End (m m)

Subtracted Initial (Installed) Displacements From Those of Final (After Tests).

Table 3.4 Dimensional Measurement for Restraints

LEFT VALUE : ORIGINAL LENGTH, RIGHT VALUE : DEVIATION AFTER TEST (m m)

	5405								5406								5407							
	R1		R2		R3		R4		R1		R2		R3		R4		R1		R2		R3		R4	
A-B	49.80	0.25	49.70	0.15	49.75	0.05	49.85	-0.05	49.95	0.2	49.80	0.1	49.90	0.05	49.95	0.05	49.70	1.05	49.70	0.45	50.00	0	49.80	0.25
B-C	50.10	0.40	50.00	0.3	49.95	0.05	50.00	0.15	49.80	0.25	50.50	0.05	49.95	0.1	50.15	0.05	50.40	0.05	50.10	0.4	50.00	0	49.70	0.1
C-D	49.60	0.35	49.70	0.1	49.90	0.05	49.70	0.1	50.00	0.3	49.70	0.1	49.75	0.1	49.70	0	49.65	1.15	49.80	0.4	49.60	0.05	50.00	0.1
D-E	49.60	0.30	49.90	0.05	49.85	-0.05	49.90	0.1	50.00	0.25	49.70	0.1	49.90	0.1	49.90	0.05	49.70	1.20	49.95	0.35	50.00	0	50.00	0
E-F	49.60	0	49.50	0	49.30	0.05	49.40	0.05	49.55	0.1	49.50	0.15	49.45	0.1	49.55	-0.05	49.70	0.85	49.60	0.3	49.60	0.1	49.40	0.2
A-F	249.40	1.35	249.70	0.25	249.60	-0.2	249.70	0	249.75	1.05	249.50	0.45	249.60	0.05	249.60	0	249.50	0.5	249.60	2.05	249.80	-0.05	249.50	0.6
A'-E'	200.00	1.20	199.90	0.35	199.85	0.15	199.90	0.15	199.90	0.75	199.95	0.45	200.00	0.2	200.00	0.3	200.00	4.5	199.70	1.6	200.00	0	199.80	0.7
G-H	49.60	0.40	50.00	0.05	49.80	0	49.95	-0.05	49.70	0.3	49.90	0.1	49.65	0.2	49.70	0.1	50.00	1.1	49.65	0.25	49.90	0.1	49.65	0.15
H-I	49.90	0.40	49.80	0.15	50.05	-0.05	49.95	0.05	50.35	0.15	50.00	0.05	50.35	0.05	49.85	0.05	49.80	1.2	50.15	0.4	50.20	0	50.30	0
I-J	49.90	0.50	49.80	0.05	50.00	0	49.95	0.1	49.60	0.25	49.90	0.1	49.70	0.1	50.00	0.05	50.10	1.4	49.95	0.4	49.80	-0.1	49.75	0.15
J-K	49.80	0.25	49.90	-0.3	49.80	0.05	49.75	0.05	49.90	0.3	49.90	0.2	49.80	0.15	50.00	0.05	50.10	1.5	49.80	0.4	49.95	-0.05	49.80	-0.4
K-L	49.50	0.15	49.40	0.2	49.35	0.05	50.15	-0.05	49.35	0.35	49.45	0.05	49.50	0.1	49.45	0	49.40	1.4	49.80	0.5	49.60	0	49.50	0
G-L	249.40	1.70	249.70	0.15	249.60	-0.2	250.30	-0.05	249.45	1.30	249.55	0.45	249.70	0.1	249.50	0.1	249.80	6.7	249.35	7.45	249.70	0.1	249.30	0.55
G'-K'	199.60	1.25	199.80	0.2	199.90	0.05	200.10	0.2	199.95	0.75	199.80	0.45	199.80	0.45	199.90	0.05	200.25	5.25	200.20	1.8	199.95	0.1	199.90	0.5
F-1	14.80	-0.20							19.60	-0.2							25.20	-0.05						
1-2	14.80	-0.3							19.80	-0.3							24.70	-0.05						
2-3	14.80	-1.0							19.35	-0.2							24.60	0.05						
3-4	14.70	-0.05							20.10	-0.15							25.00	0.2						
4-5	14.70	0.3															24.60	0.25						
4-6									40.95	-0.1														
5-6																	24.80	0.6						
5-7	29.10	0.9																						
6-7									19.40	0.55							24.15	0.65						
7-8	14.70	0.65							19.50	0.75							24.60	1.4						
8-9	14.50	0.3							19.80	0.55							24.60	1.4						
9-10	14.80	0.4							19.80	0.6							25.00	1.2						

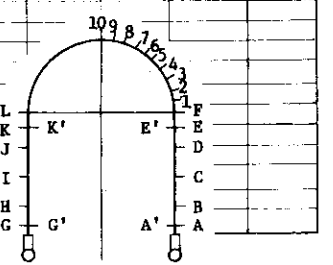

RUPTURE DISK SIDE
IS THE FACE

Table 3.5 Values of Restraint Strains in Steady State

MICRO STRAINS

LOCA-TION	5405				5406				5407			
	R1	R2	R3	R4	R1	R2	R3	R4	R1	R2	R3	R4
A	17100	2900	0	0	6000	2600	600	0	7700*	8000	0	1700
A'	17500	2600	1300	700	6400	2600	800	300	8800*	8300	1700	3100
B	14300	2600	-400	0	5100	2100	0	-900	13900*	9700	0	1600
B'	15800	2900	900	400	5400	2300	1000	1200	23800	8600	1100	2100
C	3400	-5600	-2900	-	-2100	-4500	-8600	-8400	10100	-	-	-6600
D	-	-	24300	-	-	-	-	7600	16800*	-	-	10800*

- : Over Scaled
* : Strain Gage Detached

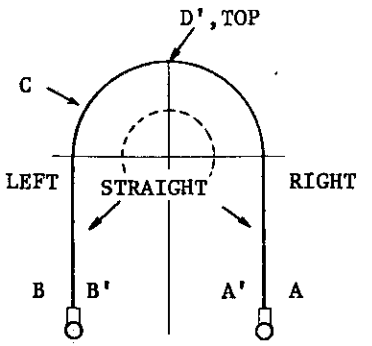

RUPTURE DISK SIDE
IS THE FACE

Table 3.6 Average Values of Restraint Strains

MICRO STRAINS

PORTION	5405				5406				5407			
	R1	R2	R3	R4	R1	R2	R3	R4	R1	R2	R3	R4
STRAIGHT	16200	2800	500	300	5700	2400	600	200	24300*	8700	700	2100
TOP	27000*	-	24300	-	30300*	-	-	7600	56900*	-	-	-

* : From Dimensional Measurements
- : Not Measured in Dim. Meas. And/or Strain Gage Detached
Others : Averaged From Four Strain Gages in STRAIGHT Portion

Table 3.7 Peak Value of Restraint Strain and Peak Time

(MICRO STRAIN/mSEC. PASSED AFTER COLLISION)

* : Ref. Data (Strain Gage Failed)
** : " (Peak of Bending Vibration)

LOCA-TION	5405				5406				5407			
	R1	R2	R3	R4	R1	R2	R3	R4	R1	R2	R3	R4
A	14600/11.7	5100/8.2	2100/8.7**	1400/11.2**	6200/7.0	4000/6.8	2300/10.3	-2400/8.0**	18200/6.7*	10400/13.7	3900/1.5	5000/9.2
A'	14600/13.0	5700/5.0	4300/4.5	4000/5.7	6600/6.0	4600/6.0	3400/6.8	2800/8.3**	18900/6.2*	10100/6.2	4000/6.0	6100/6.5
B	11700/12.0	4400/11.7	—	-2300/6.2**	4700/7.5	3600/6.5	1900/8.3	-1900/17.5**	21600/9.0	11900/7.8	2100/10.0	4900/9.0
B'	13700/12.2	5000/4.5	—	2600/5.7	4900/7.0	3600/6.0	3300/6.5	2600/7.0**	21200/6.2	10600/6.2	4300/7.2	5300/6.5
C	-4600/1.5	-6600/7.7	-3400/9.5**	—	-6400/6.0	-4300/5.8	-9300/9.8	-9900/11.5	-10300/4.5	-10000/4.0*	-10300/5.0*	-11700/4.8
D	19900/2.2*	—	—	—	18200/3.0*	22900/2.8*	—	14300/3.5*	27900/3.2*	31100/0.7*	24300/1.0*	42900/1.2*

Table 3.8 Average Values of Peak Restraint Strains at Straight Portion

(MICRO STRAINS/mSEC. PASSED AFTER COLLISION)

	5405				5406				5407			
	R1	R2	R3	R4	R1	R2	R3	R4	R1	R2	R3	R4
STRAI.R	11700/5.2	4000/5.0	2000/4.7	1100/5.7	6100/6.8	4000/6.5	2100/6.8	700/7.0	—	8600/6.0	2300/6.2	4700/6.5
STRAI.L	8900/5.2	3900/4.5	—	1100/4.5	4700/7.3	3400/6.8	1700/6.4	700/6.0	21200/6.2	9700/6.0	2600/6.7	4100/6.5
MEAN	10300	4000	2000	1100	5400	3700	1900	700	21200	9200	2500	4400

Table 4.1 Peak Value of Restraint Force

	5405		5406		5407	
	Strain	Force	Strain	Force	Strain	Force
R1	0.0103	4.1	0.0054	4.0	0.0212	4.3
R2	0.004	3.9	0.0037	3.9	0.0092	4.1
R3	0.002	3.8	0.0019	3.8	0.0025	3.8
R4	0.0011	2.2	0.0007	1.4	0.0044	3.9
Total		14.0		13.1		16.1

R : Right Side

L : Left Side

Strain : Micro Strains

Force : Ton

Table 4.2 Absorbed Strain Energy

(kgf-m)

		5405		5406		5407	
		ε_0	S.E.	ε_0	S.E.	ε_0	S.E.
RESTRAINT	R1	0.0162	27.6	0.0057	9.9	0.0243	53.1
	R2	0.0028	4.4	0.0024	4.0	0.0087	18.1
	R3	0.0005	0	0.0006	0	0.0007	0
	R4	0.0003	0	0.0002	0	0.0021	4.1
	Total		32.0		13.9		75.3
PIPE S.E.		172.2		72.1		534.5	
EXTERNAL WORK		324		343		1069	

S.E.: Strain Energy kgf-m

ε_0 : Strain mm mm

External Work : Average Work Done By Thrust Force.

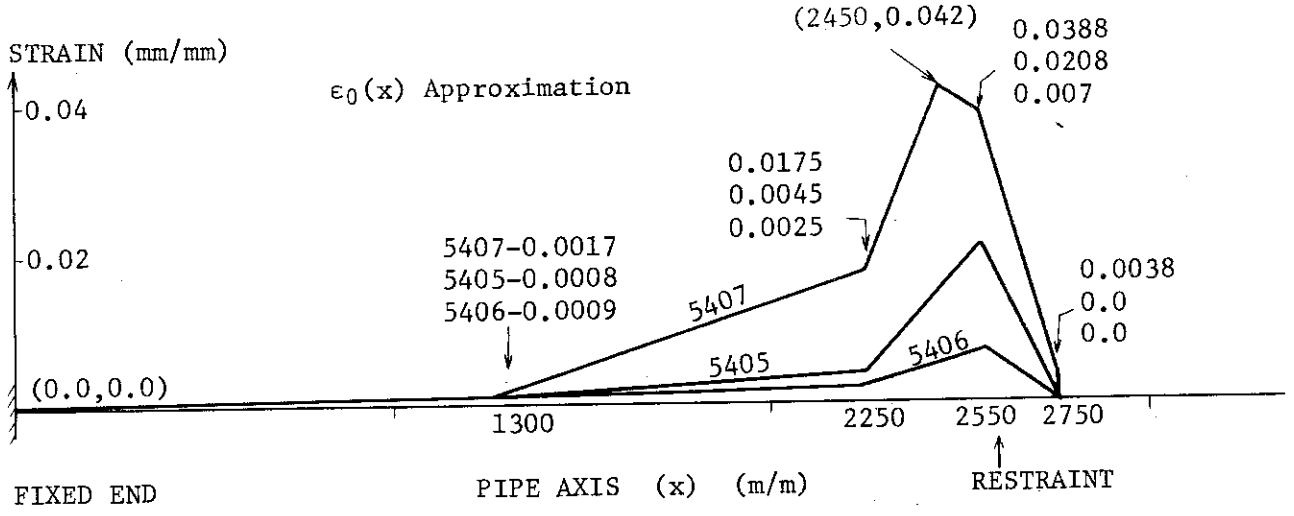

Table A1 Experimental Value of Characteristic Period

Clearance	Direction of Excitation	Period (msec)	
		1st Mode	2nd Mode
30	Upward	95	—
50	Upward	98	14
100	Transverse	101	13.5
	Upward	108	16

Table A2 Calculated Results of National Period of Restraints

Clearance(mm)	Period (msec)				
	1st mode	2nd mode	3rd mode	4th mode	5th mode
30	65.9	12.8	8.1	3.9	2.7
50	71.5	13.9	8.7	4.3	2.9
100	86.2	16.8	10.1	5.6	3.6
100 *	47.7	18.2	10.5	5.7	4.1

* Note this calculation was done for deformed shape

Table A3 Calculated Results of Natural Period of Test Pipe

Case	Calculational Conditions				Period (msec)				
	Consistent Mass	Number of Mesh	Condition at R Point	Freedom in Y-direction	1st Mode	2nd Mode	3rd Mode	4th Mode	5th Mode
1	existence	15	Pin Supporting	No	16.5	6.2	3.7	2.1	1.3
2	none	15	Pin Supporting	No	16.5	6.2	3.7	2.1	1.3
3	none	15	Dumper	No	103.5	16.1	5.7	2.9	1.7
4	none	30	Pin Supporting	No	16.4	6.1	3.6	2.1	1.3
5 *	none	15	Pin Supporting	Yes	10.2	4.5	3.2	1.9	1.2

* Calculation in Case 5 was performed with regard to the deformed shape.

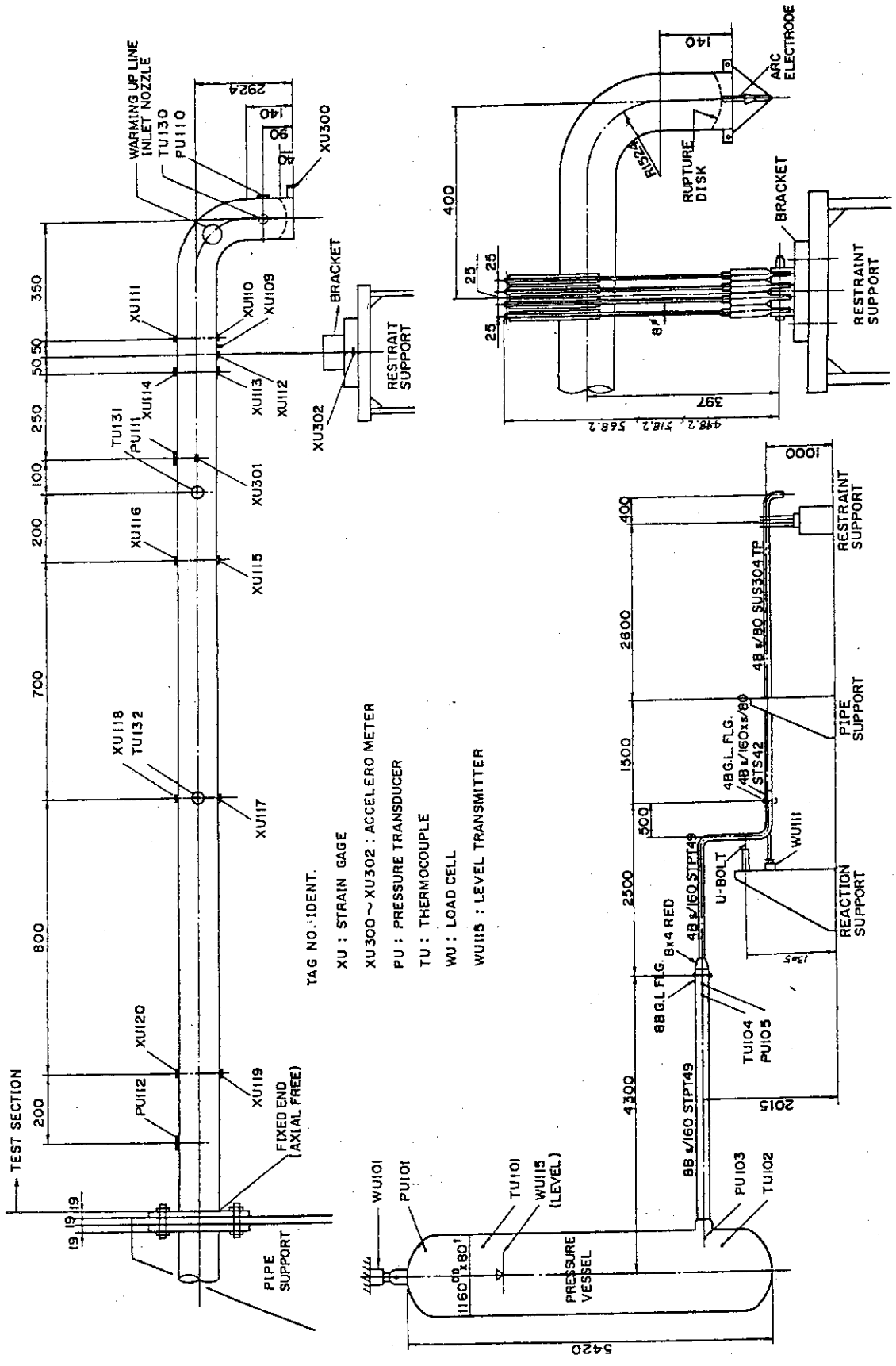

Fig.2.1 Schematic of Pipe Whip Test

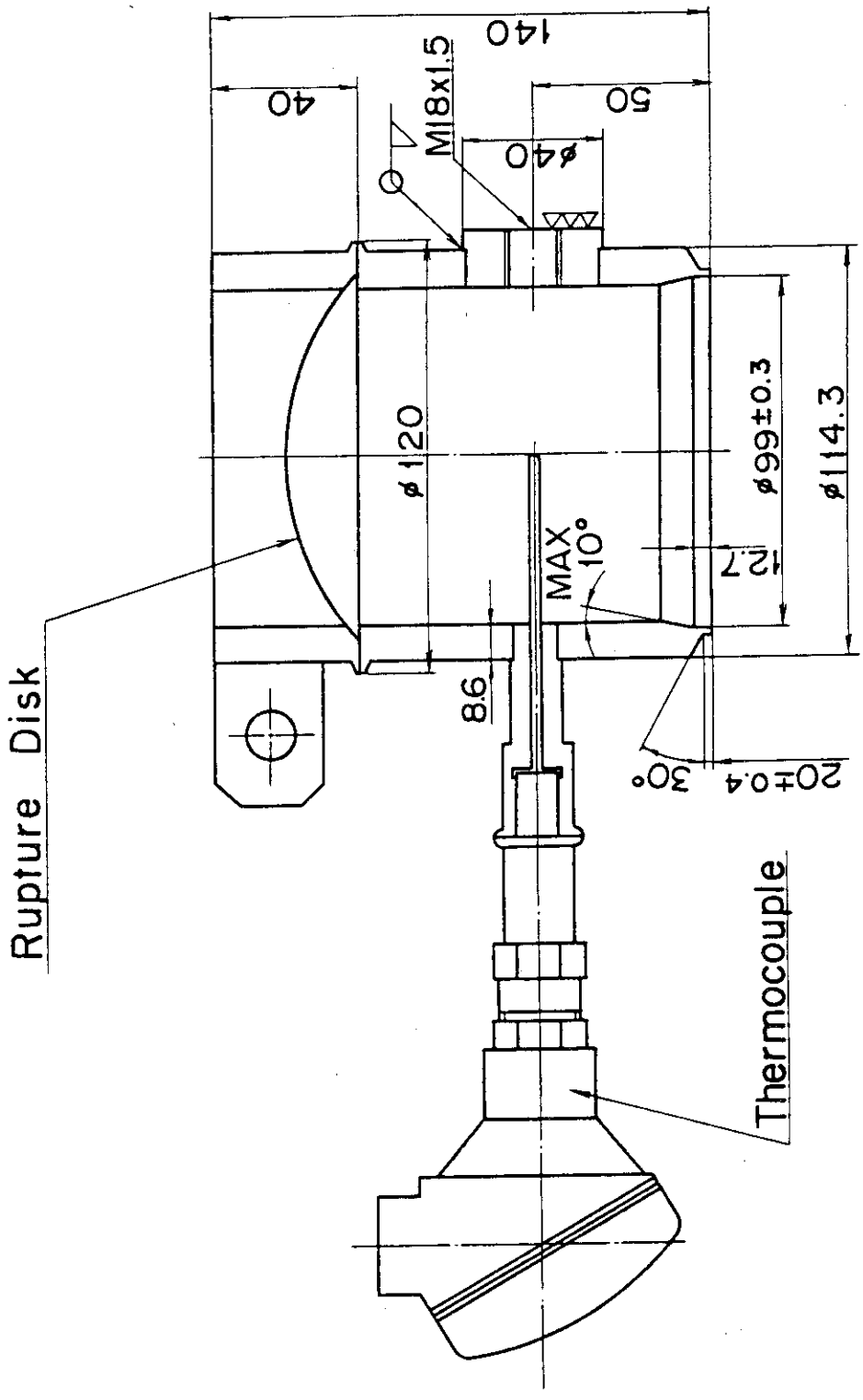

Fig.2.2 Details of Welded Type of Rupture Disk

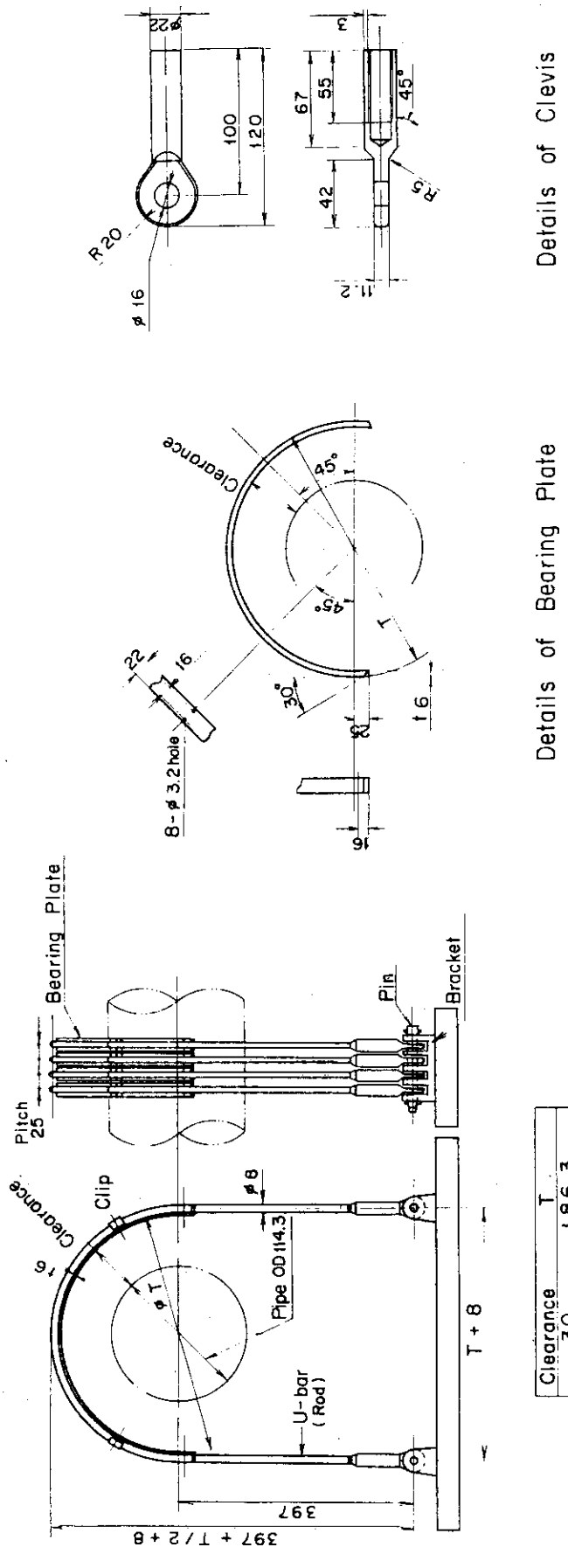

Fig. 2.3 Restraint Configuration

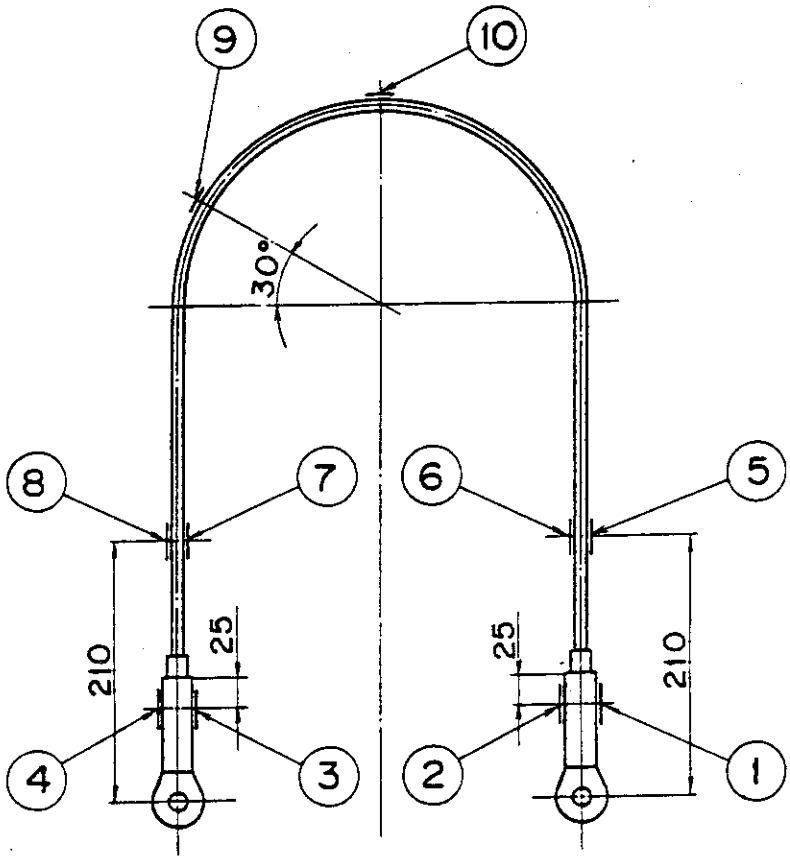

Location	Tag Number			
	Restraint 1	Restraint 2	Restraint 3	Restraint 4
①	XU 121	XU 131	XU 141	XU 151
②	122	132	142	152
③	123	133	143	153
④	124	134	144	154
⑤	125	135	145	155
⑥	126	136	146	156
⑦	127	137	147	157
⑧	128	138	148	158
⑨	129	139	149	159
⑩	130	140	150	160

Fig.2.4 Locations of Strain Gages on Restraints

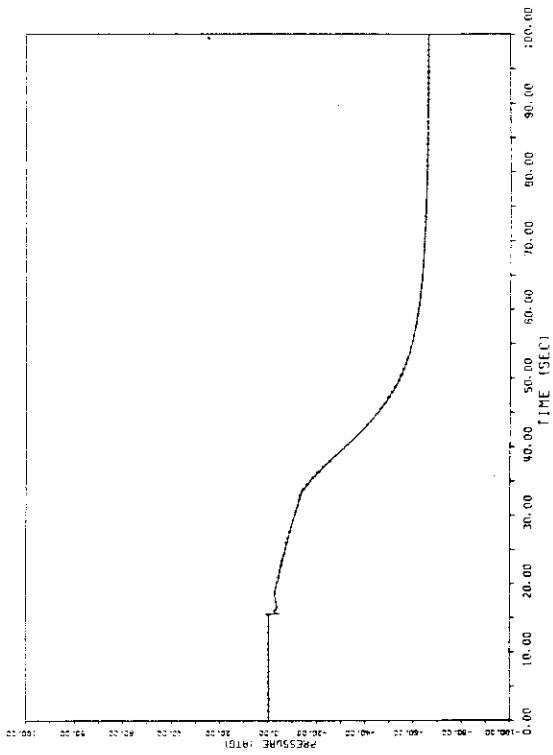

Fig.3.1 Pressure-Time History in Pressure Vessel (Long Term)
(RUN 5407, PU 101, 0-100 sec)

Fig.3.2 Pressure-Time History in Nozzle (Long Term)
(RUN 5407, PU 105, 0-100 sec)

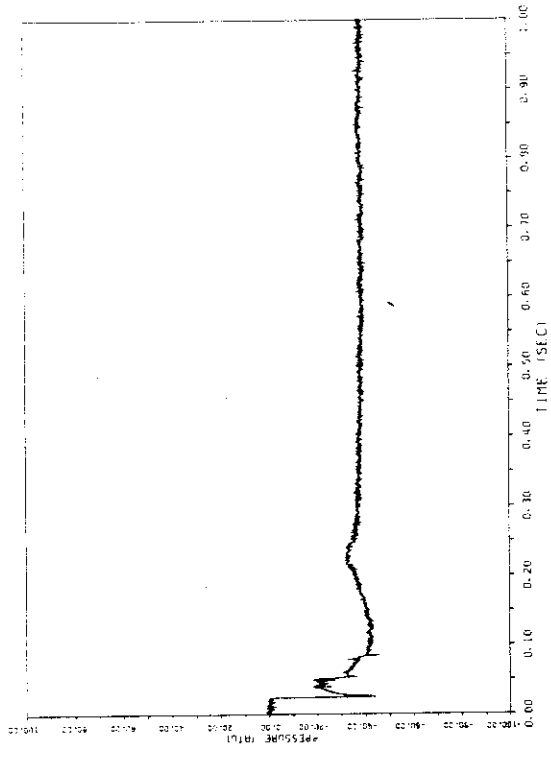

Fig.3.3 Pressure-Time History in Test Pipe (Short Term, PU 110)
(RUN 5406, PU 110, 0-1 sec)

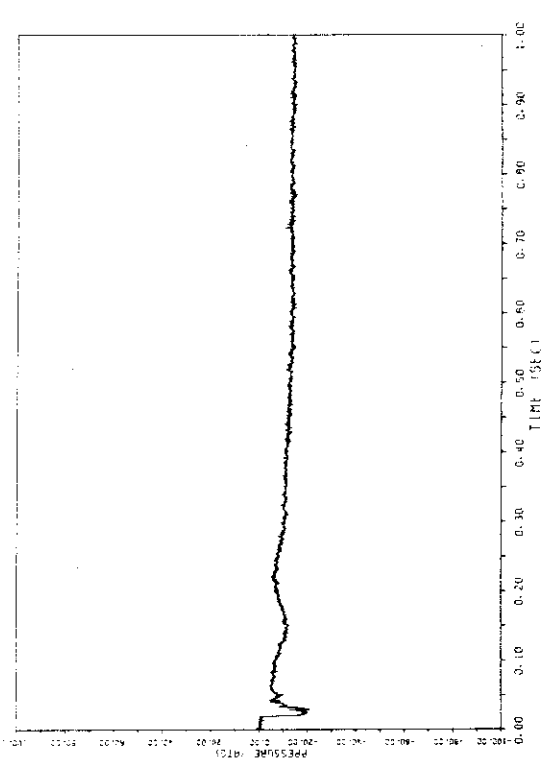

Fig.3.4 Pressure-Time History in Test Pipe (Short Term, PU 111)
(RUN 5405, PU 111, 0-1 sec)

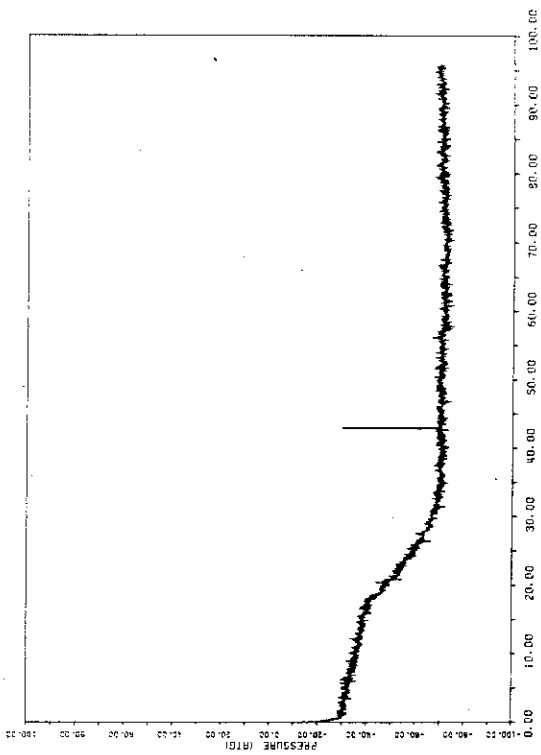

Fig.3.5 Pressure-Time History in Test Pipe (Short Term, PU 112)
(RUN 5406, PU 112, 0-1 sec)

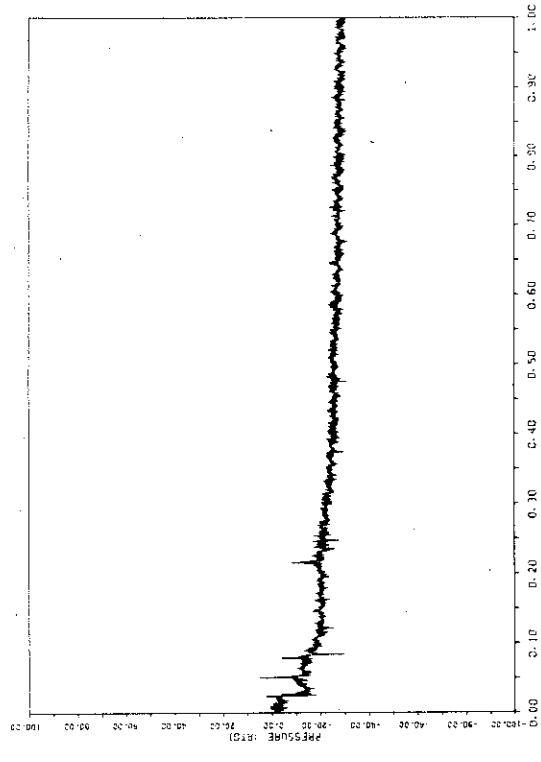

Fig.3.6 Pressure-Time History in Test Pipe (Long Term, PU 112)
(RUN 5406, PU 112, 0-100 sec)

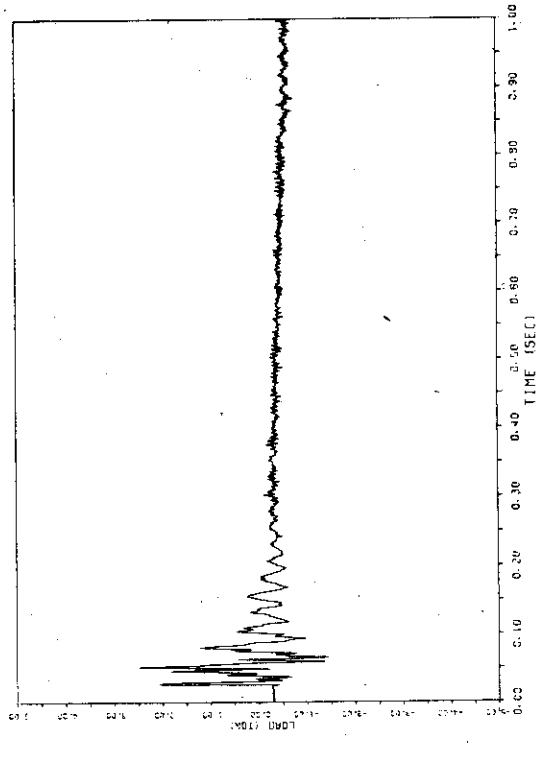

Fig.3.7 Force-Time History at Second Elbow
(RUN 5406, WU 111, 0-1 sec)

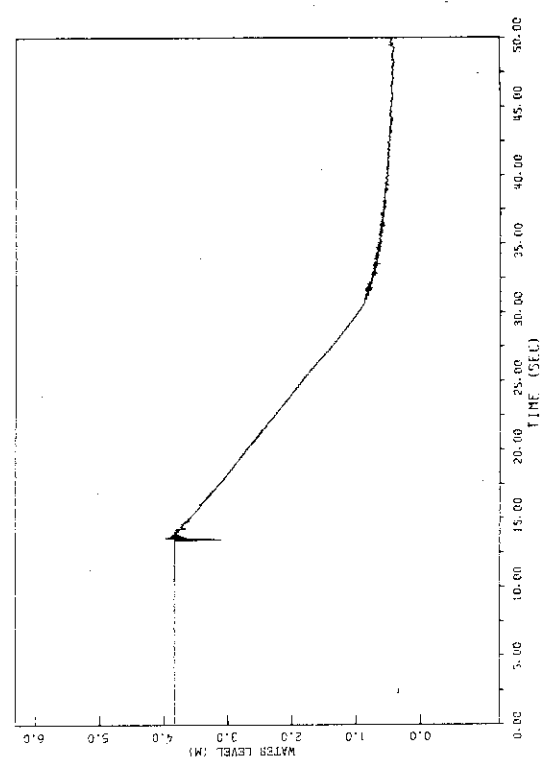

Fig.3.8 Variation of Fictious Water Level
(RUN 5405, SU 115, 0-50 sec)

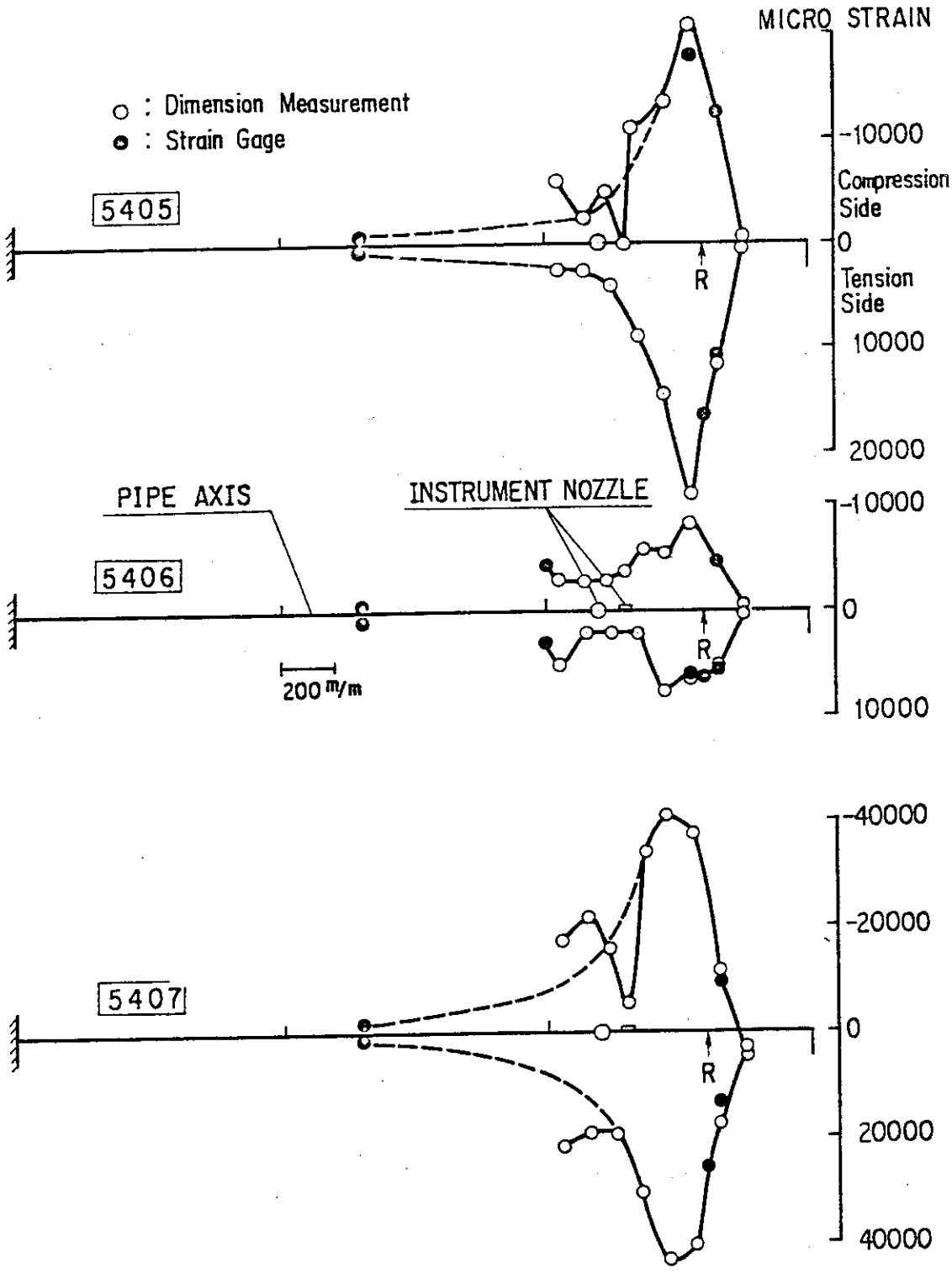

Fig.3.9 Distribution of Residual Pipe Strain

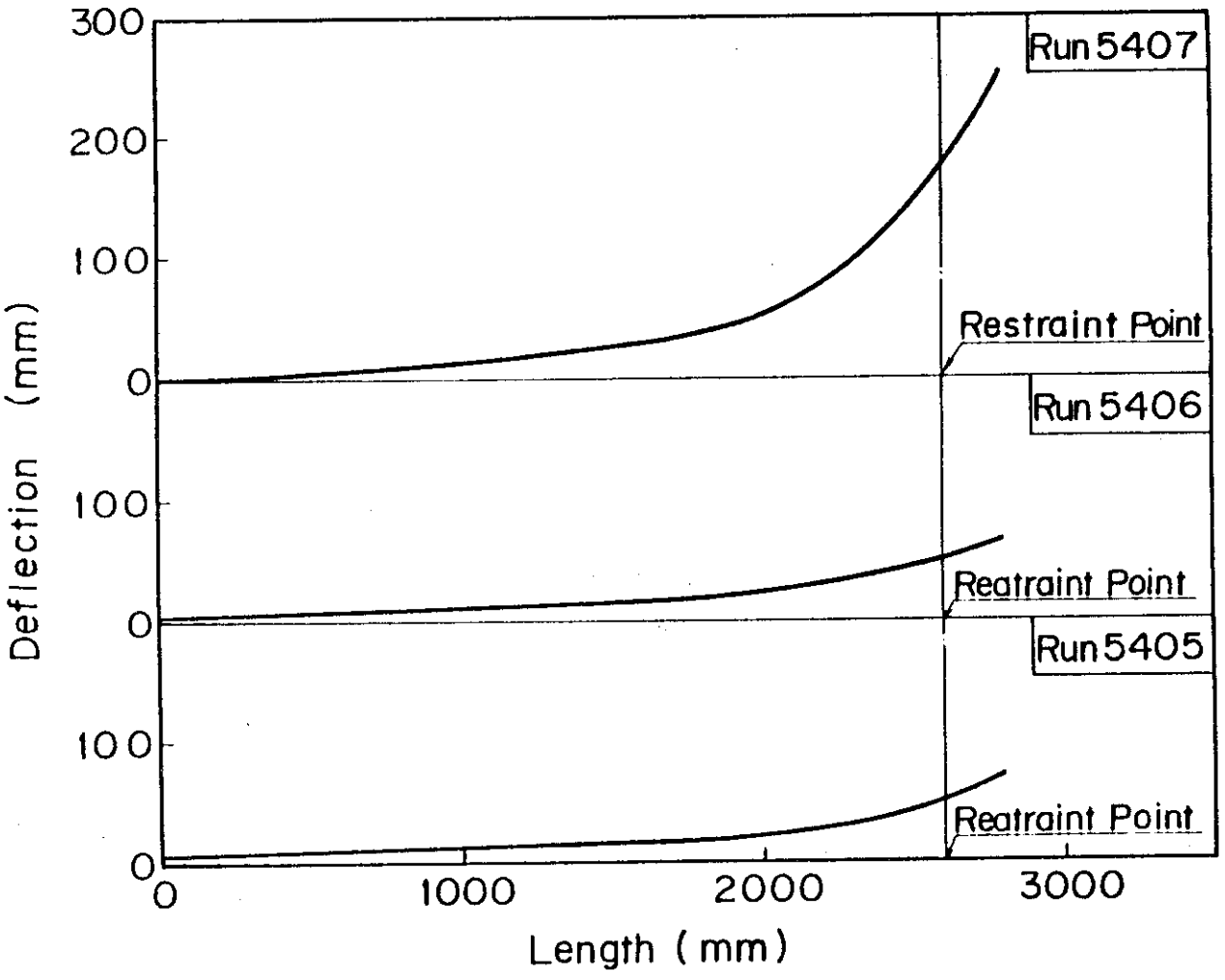

Fig.3.10 Residual Displacement of Test Pipe

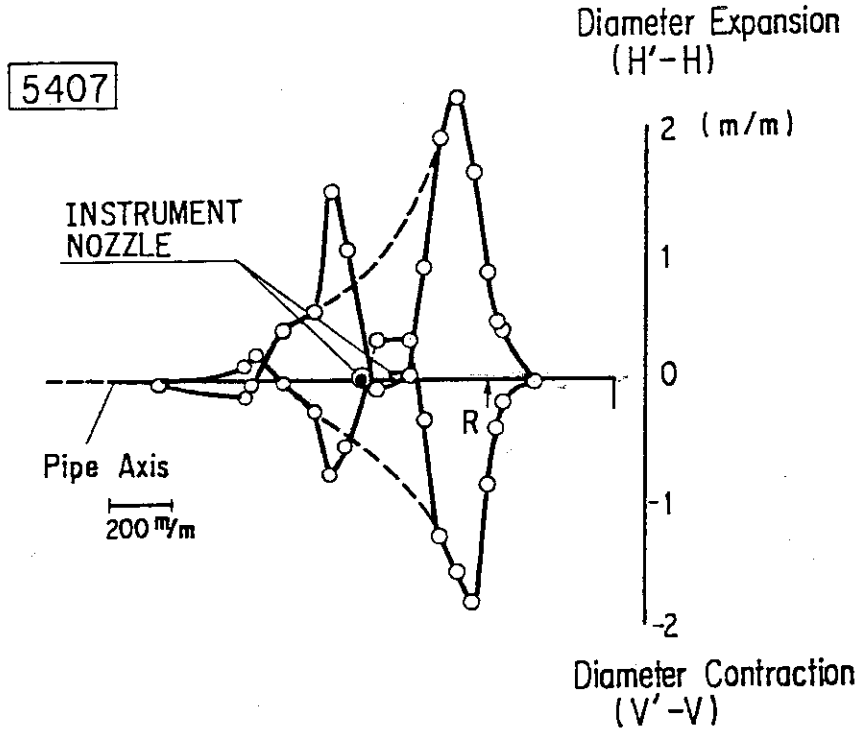

(m/m)

L		250		350		370		400		450		500		550	
H	V	4.10	3.94	4.08	4.03	a	b	a	b	4.03	4.07	a	b	4.06	4.07
H'	V'	4.06	3.91	4.47	3.84	4.55	3.60	4.90	3.20	5.67	2.28	6.30	2.50	5.98	2.80

600		650		750		850		900		950		1050	
a	b	4.76	3.15	3.99	3.64	2.97	4.71	a	b	4.04	4.12	4.03	4.03
5.30	3.25	4.77	3.46	3.90	3.95	4.01	4.16	5.00	3.65	4.58	3.85	4.42	3.99

1150		1375		1450		2550		2850		2950		3000	
4.00	4.25	3.90	4.15	4.00	4.00	3.85	4.00	3.85	4.25	3.85	4.05	4.00	3.90

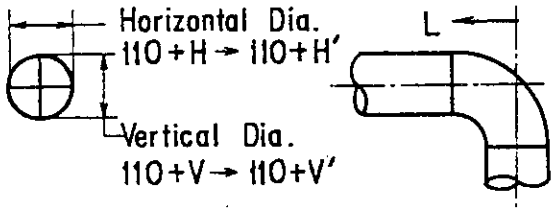

a : Not measured. Used mean value of before and behind H.
b : 〃 〃 V.
Other Blank : Not measured.
Used mean value of L=350, 450 550, 950, 1050 of H and V resp.

Fig.3.11 Ovallization of Test Pipe

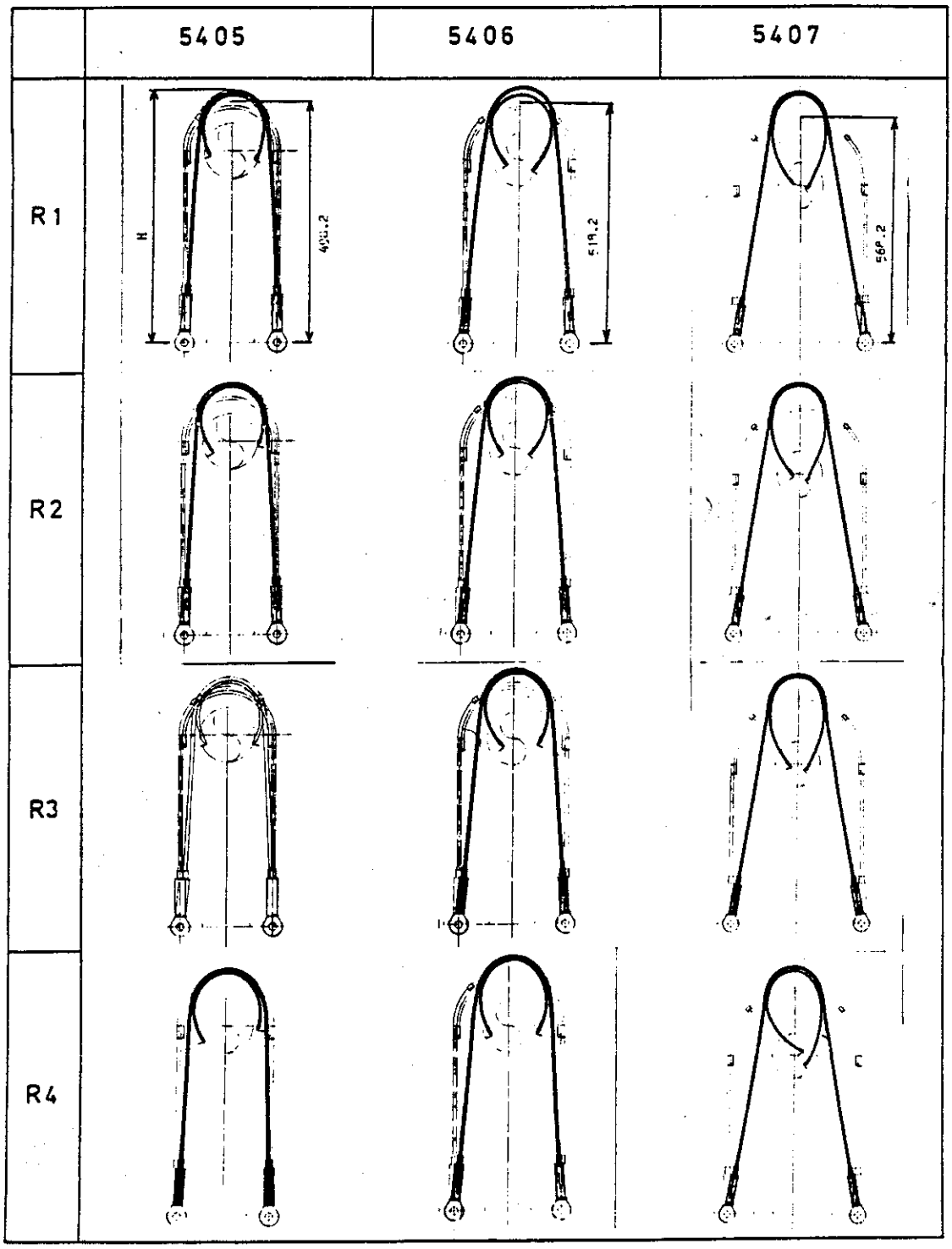

H DIMENSION

	5405	5406	5407
R1	522.1	561.0	658.0
R2	519.4	560.9	653.3
R3	517.1	547.8	650.2
R4	515.7	546.8	646.8

(m/m)

NET ELONGATION

	5405	5406	5407
R1	7.8	7.8	43.7
R2	5.1	5.8	39.0
R3	3.8	3.7	35.9
R4	1.4	2.7	32.5

(m/m)

Fig.3.12 Deformation of Restraints

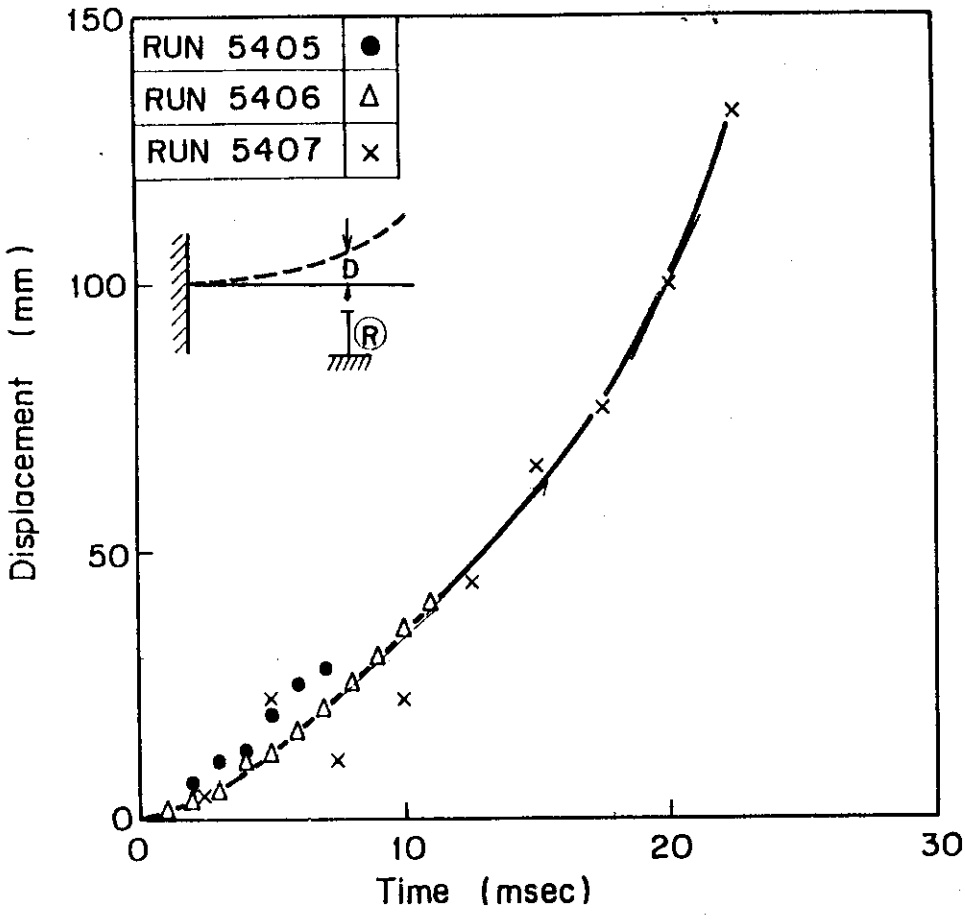

Fig.3.13 Displacement-Time History at Restraints Measured by High Speed Camera

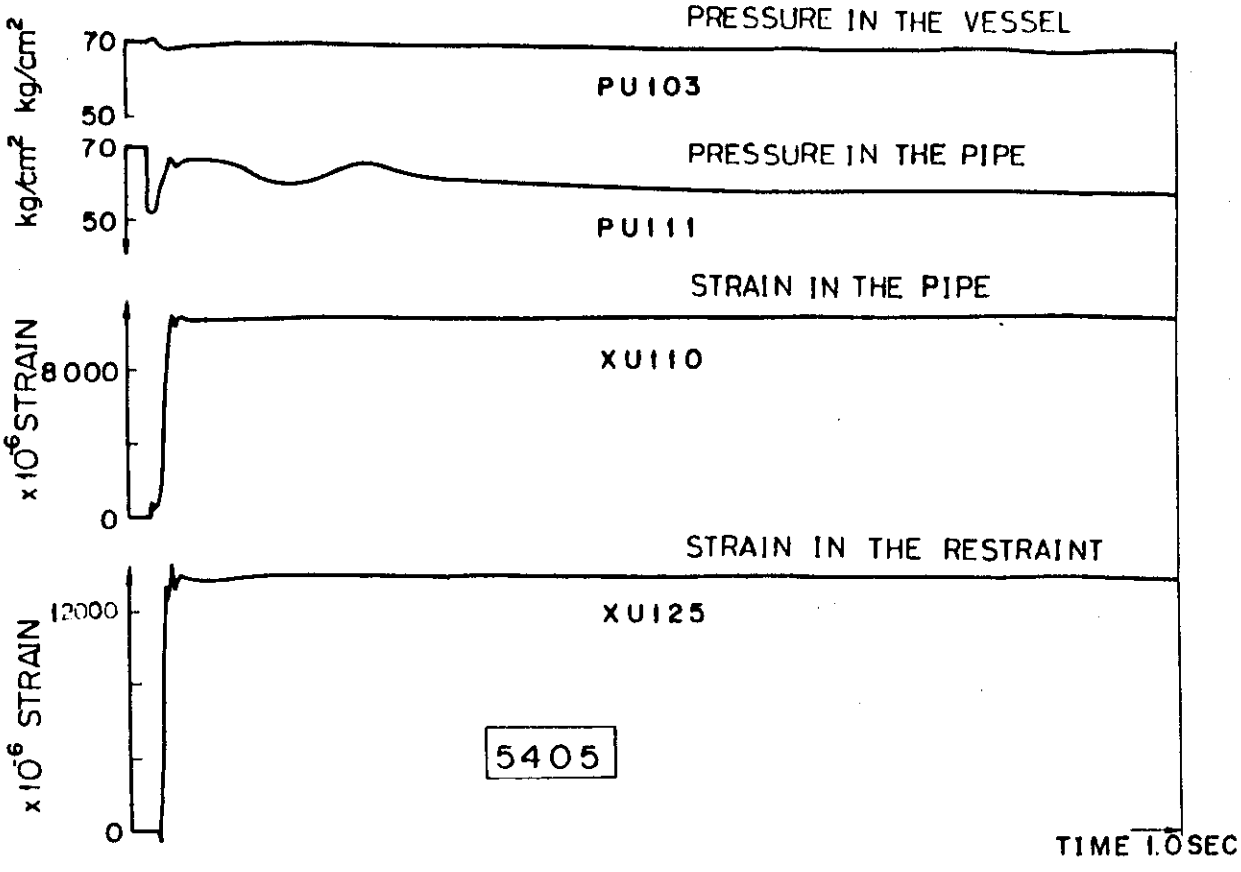

Fig.4.1 Comparison between Pressure-and Strain-Time Histories

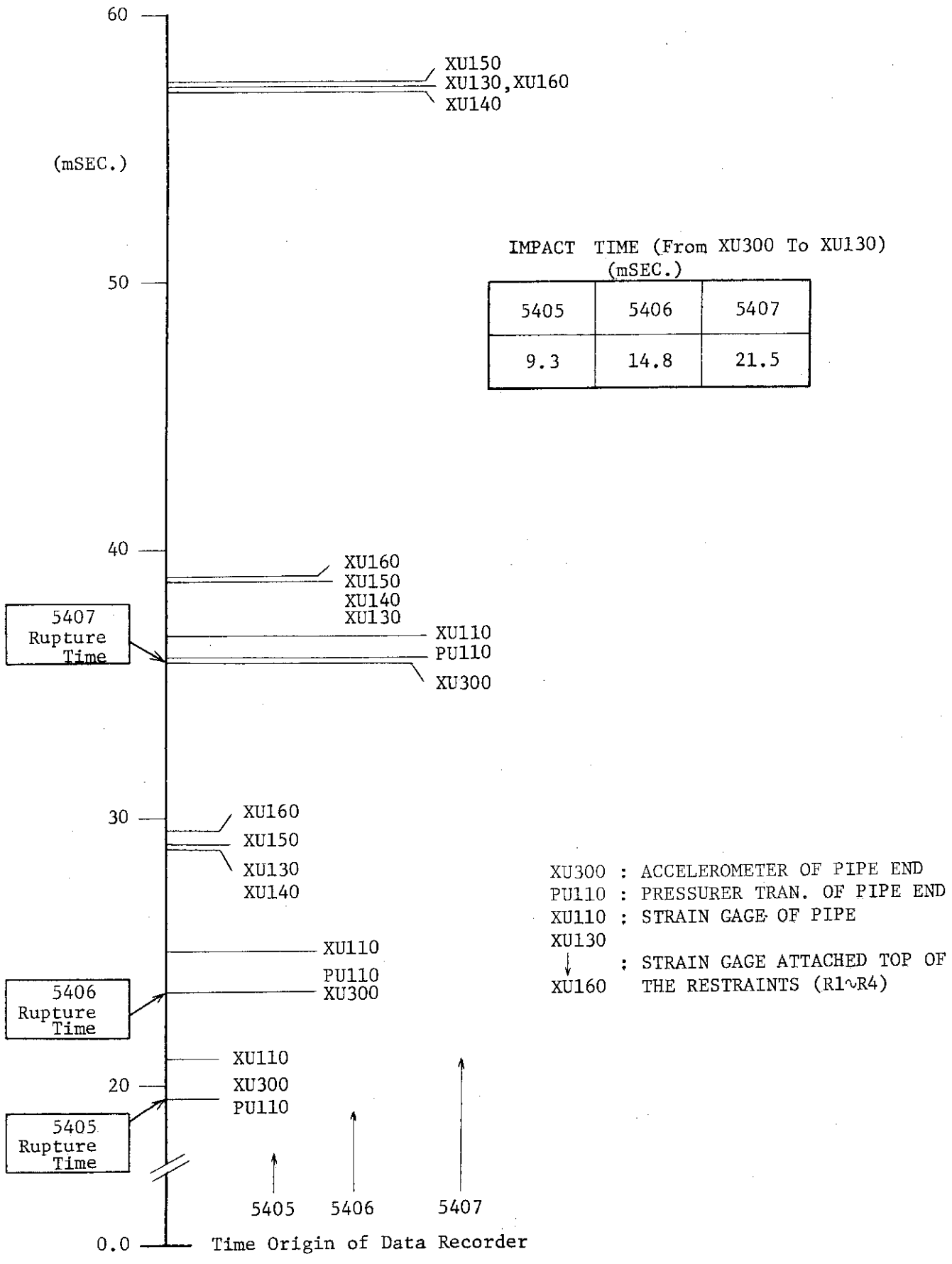

IMPACT TIME (From XU300 To XU130)
(mSEC.)

5405	5406	5407
9.3	14.8	21.5

XU300 : ACCELEROMETER OF PIPE END
PU110 : PRESSURER TRAN. OF PIPE END
XU110 : STRAIN GAGE OF PIPE
XU130
↓ : STRAIN GAGE ATTACHED TOP OF
XU160 THE RESTRAINTS (R1∿R4)

Fig.4.2 Time Sequence of Major Events

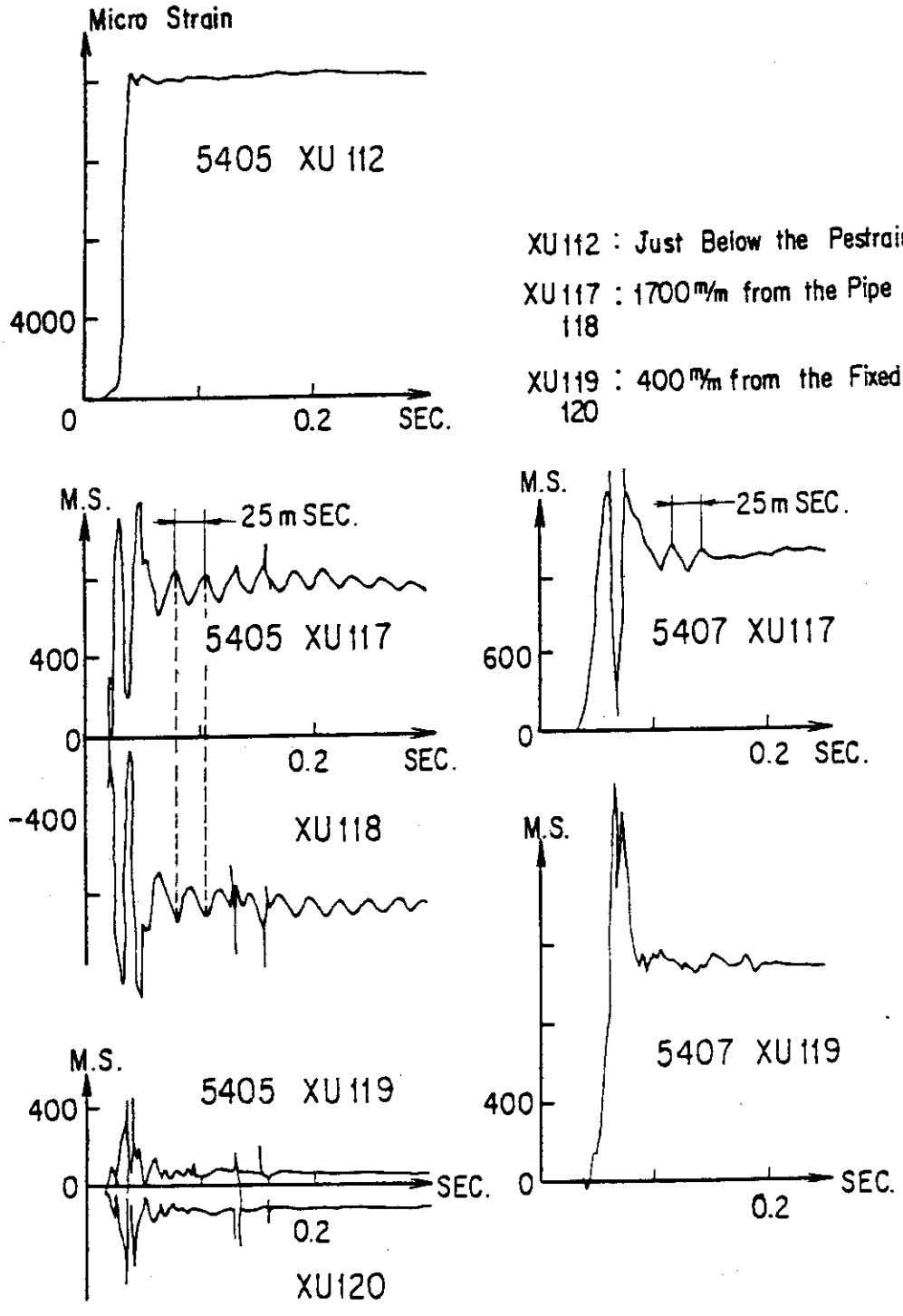

Fig.4.3 Strain-Time Histories in Test Pipe

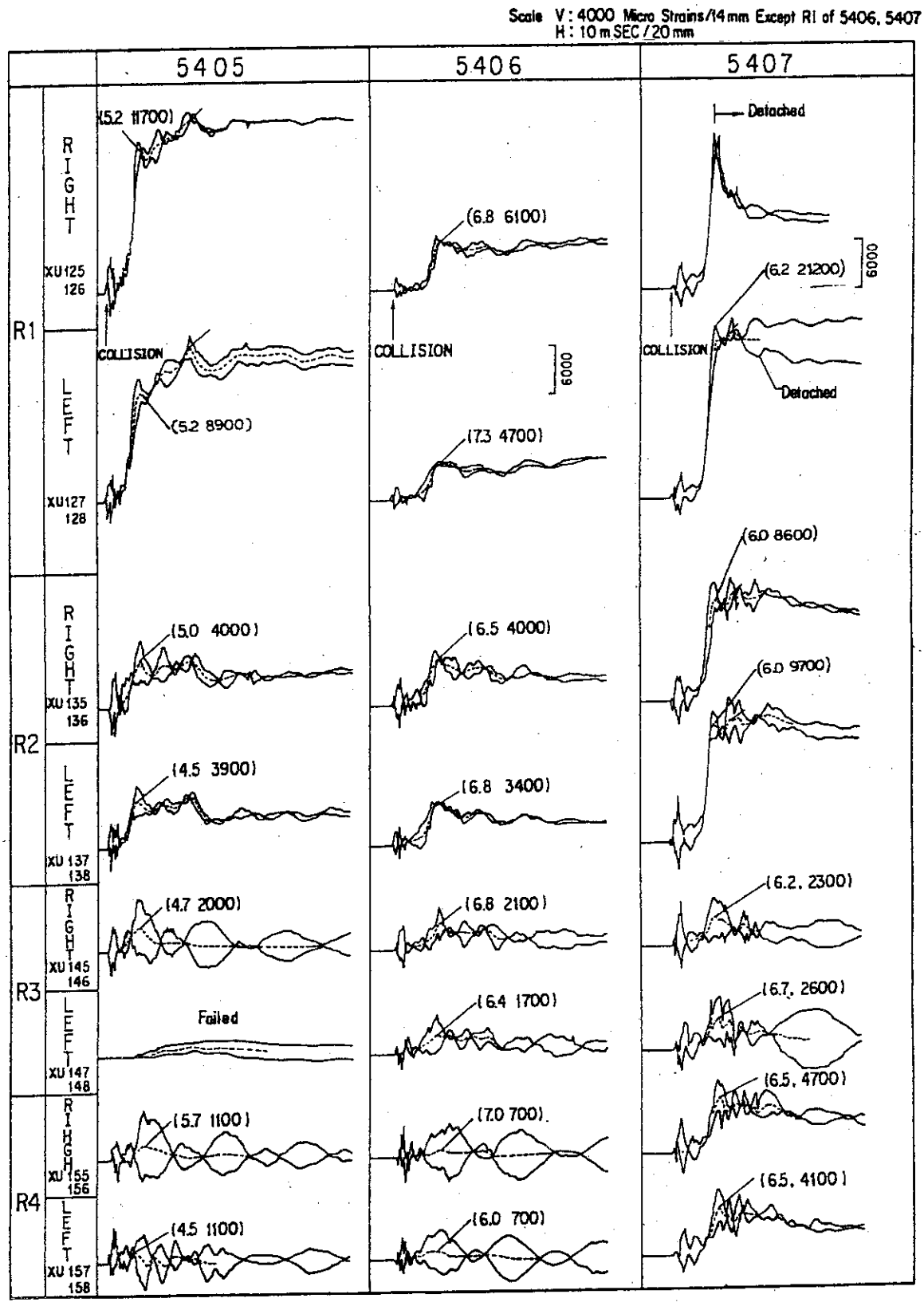

Fig.4.4 Strain-Time Histories at Straight Portion of Restraint

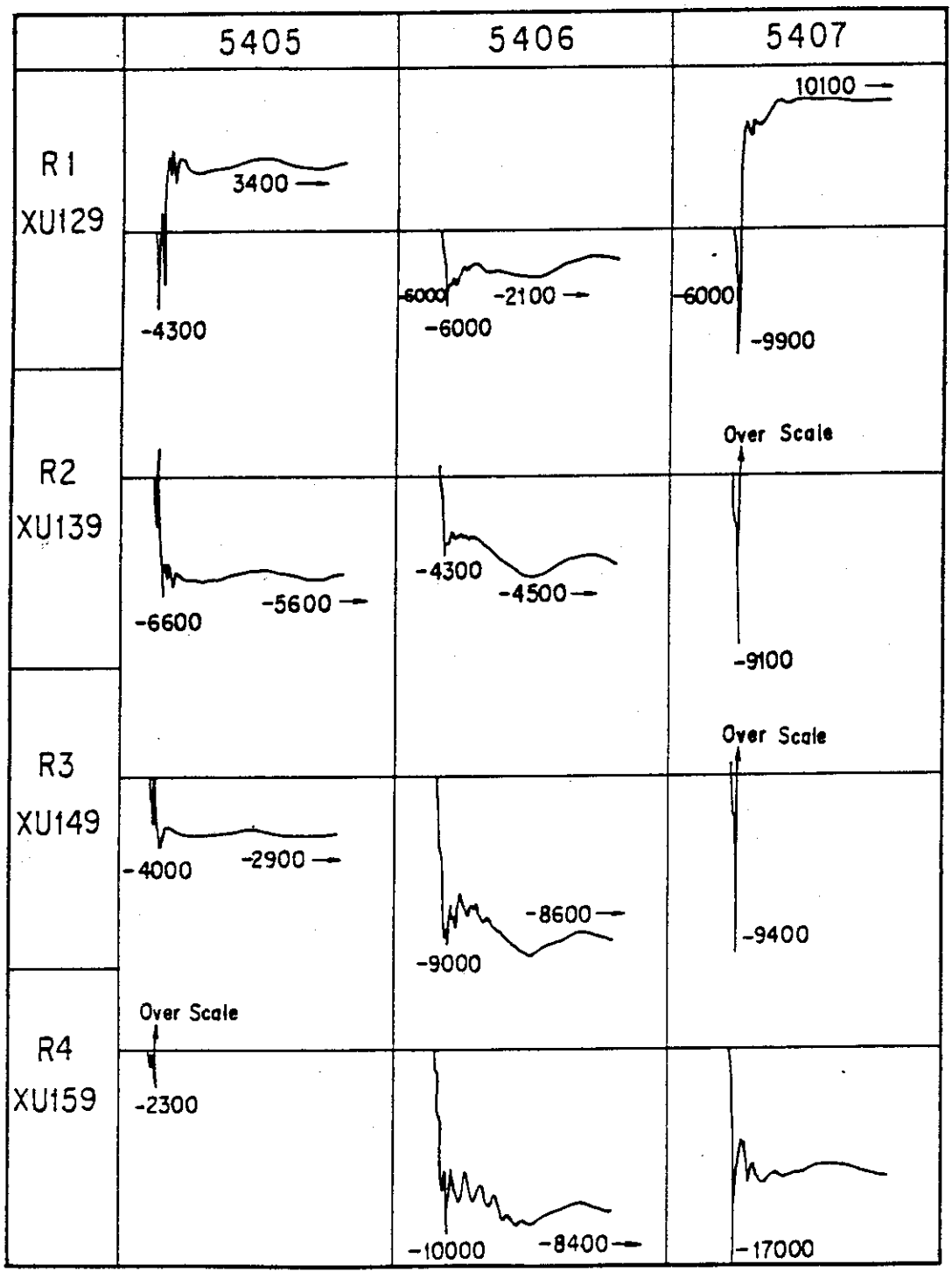

Fig.4.5 Strain-Time Histories at Circular Portion of Restraint

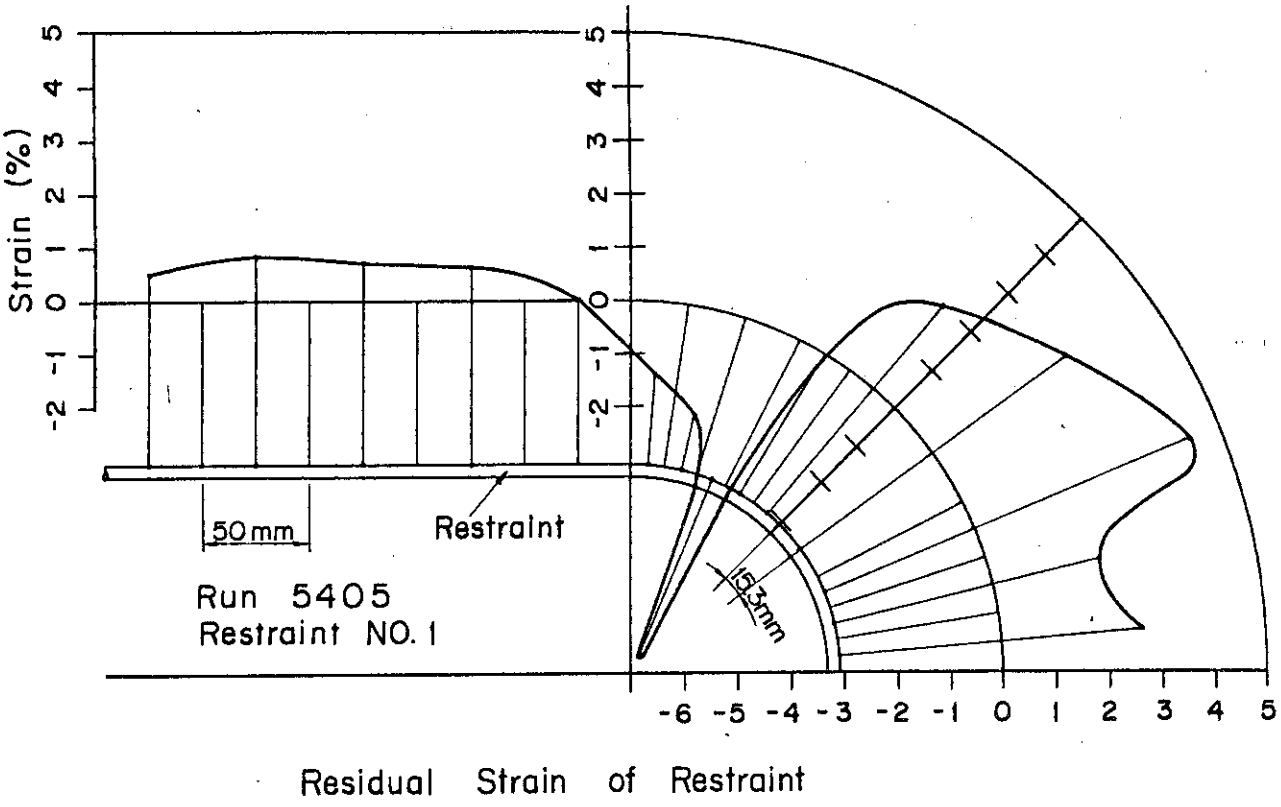

Fig.4.6 Residual Strain Distribution of Restraints (Run 5405)

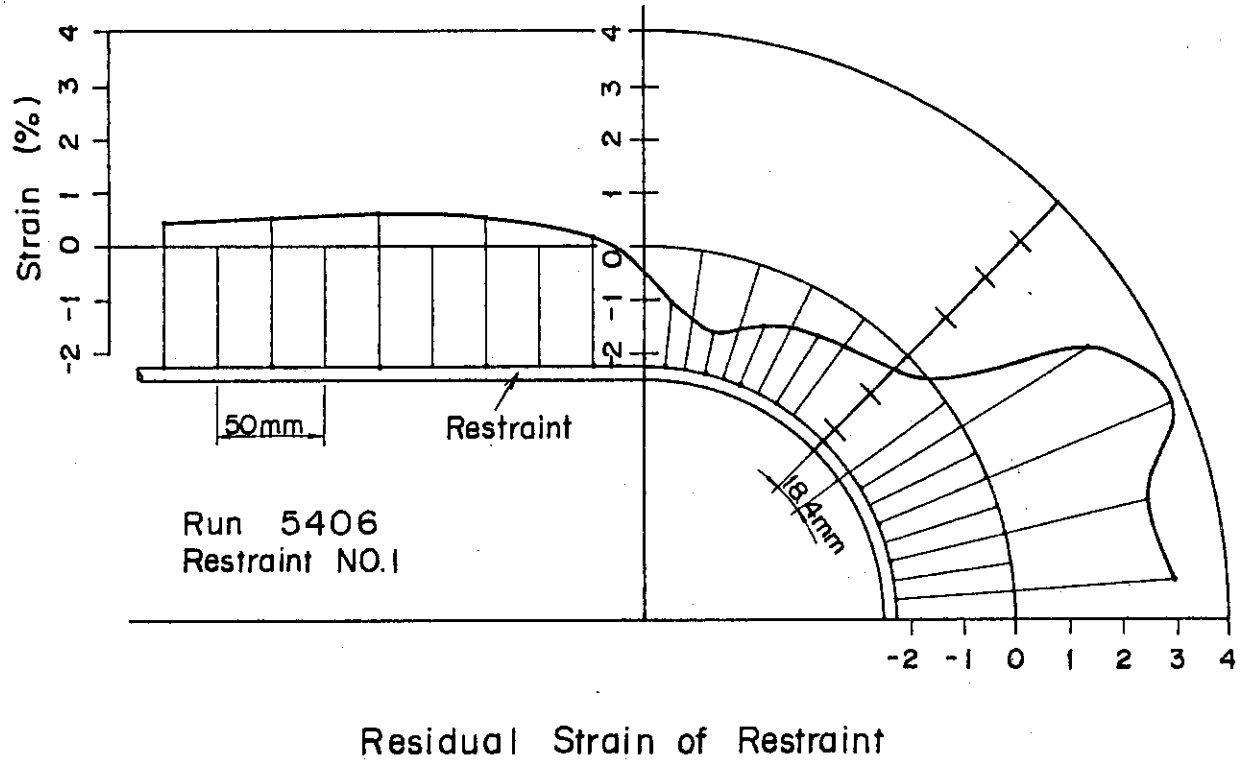

Fig.4.7 Residual Strain Distribution of Restraints (Run 5406)

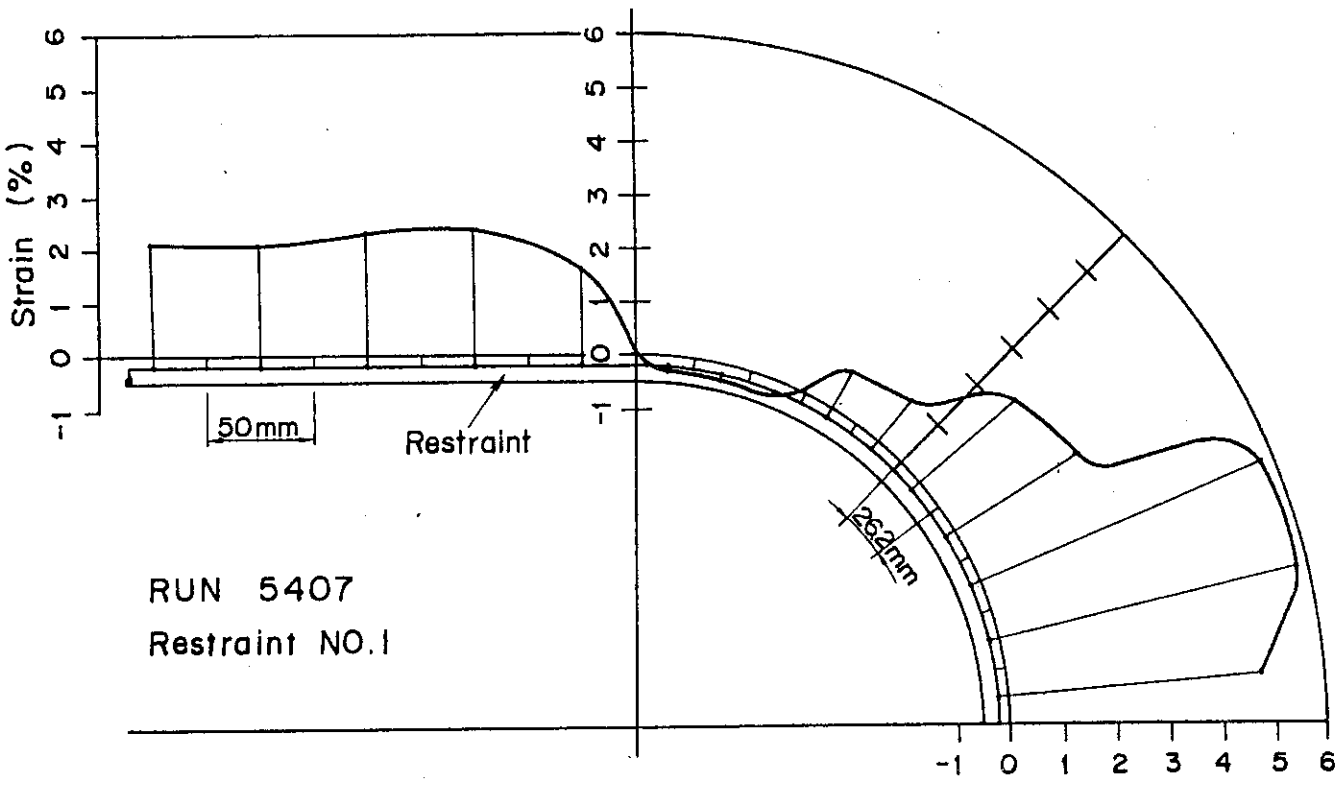

Fig.4.8 Residual Strain Distribution of Restraints (Run 5407)

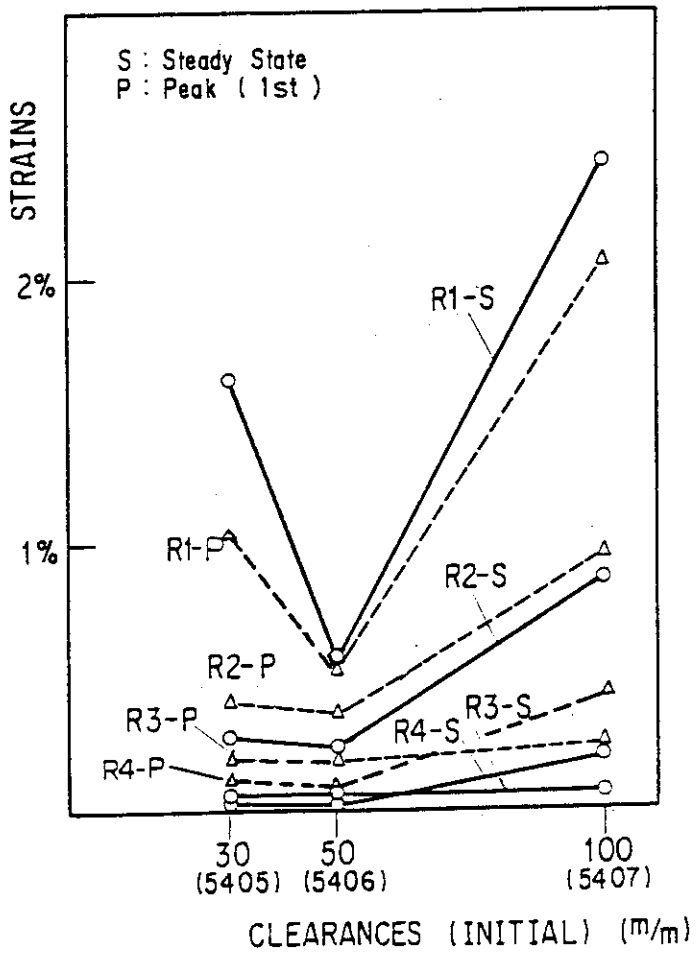

Fig.4.9 Restraint Strain at Straight Portion Versus Clearance

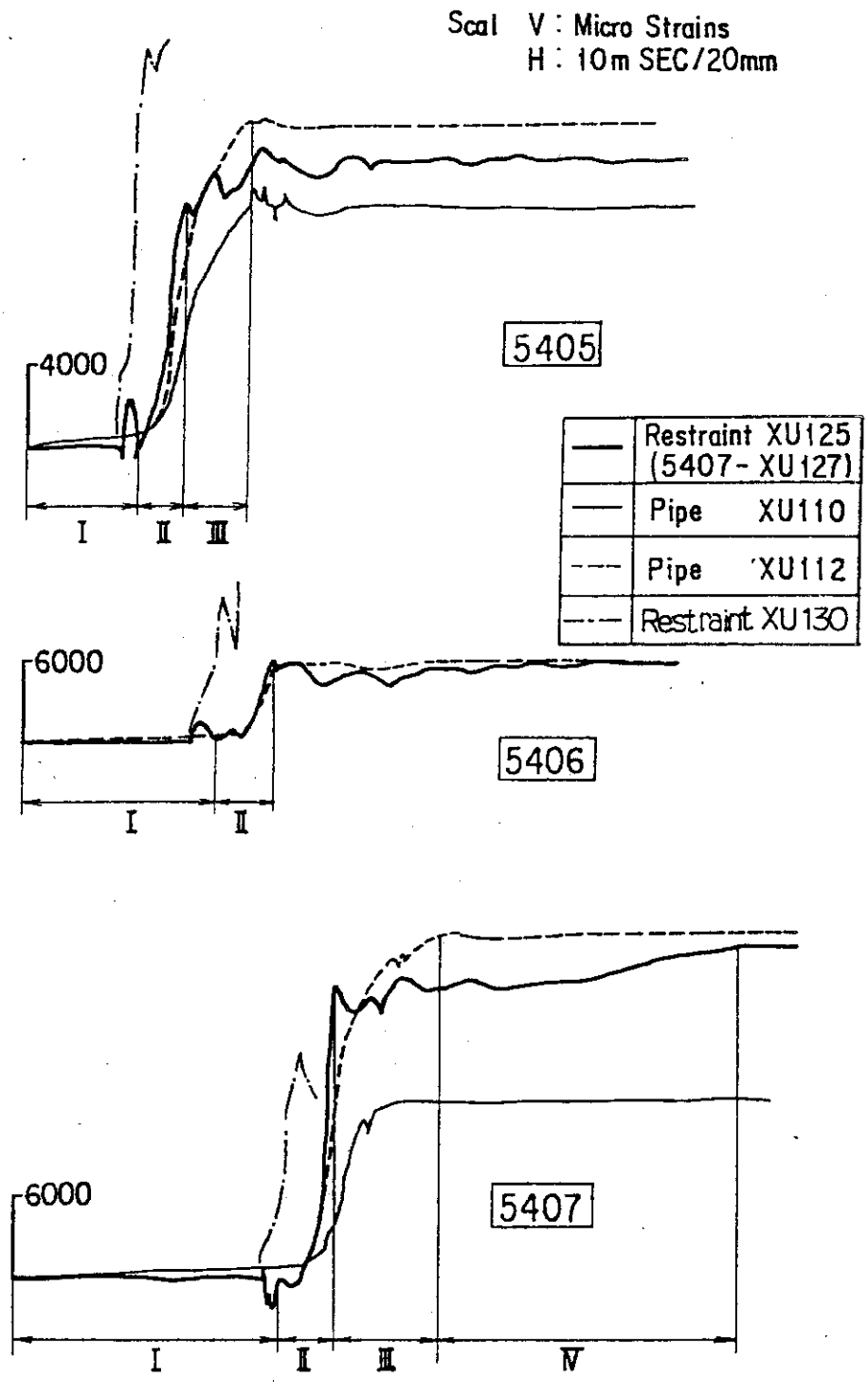

Fig.4.10 Comparison between Pipe Strains and Restraint Strains

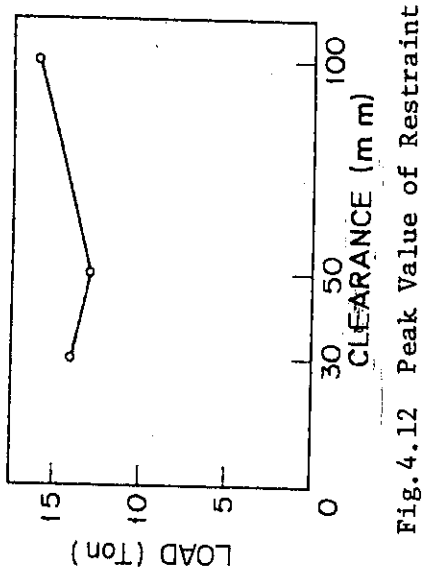

Fig.4.12 Peak Value of Restraint Force

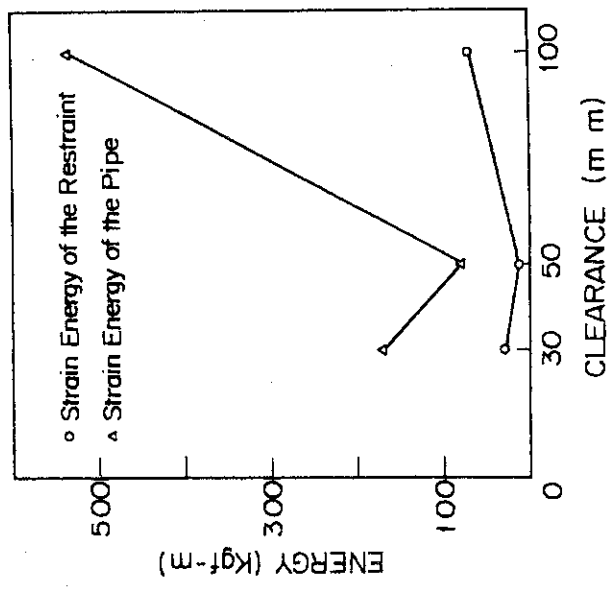

Fig.4.13 Absorbed Strain Energy

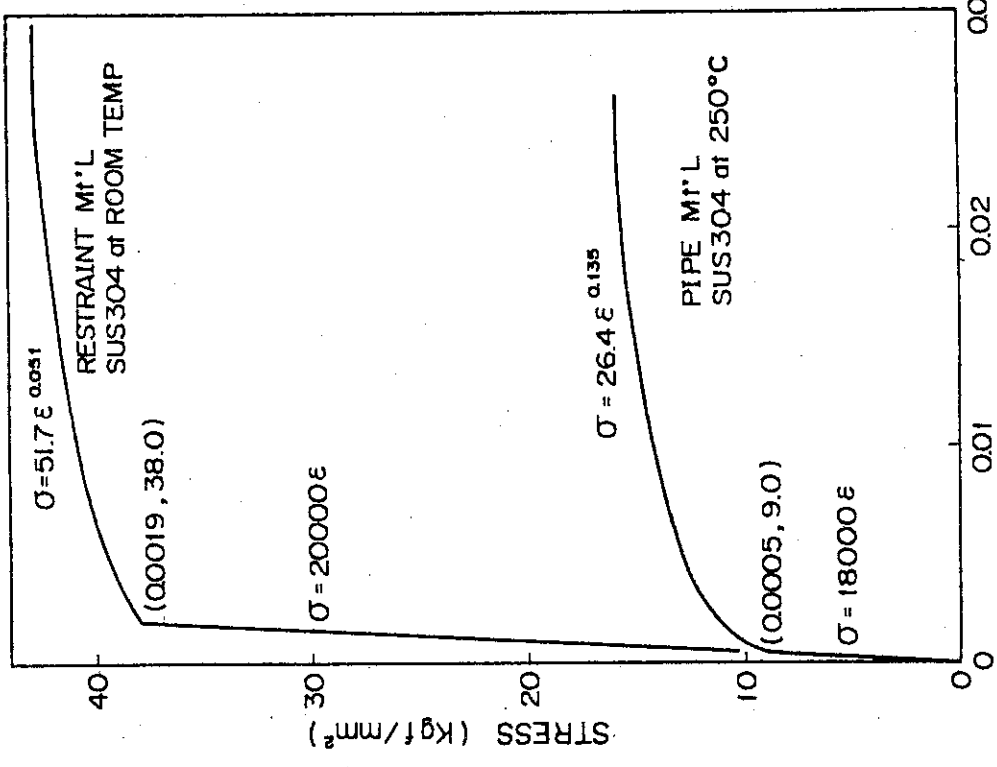

Fig.4.11 Stress-Strain Relationship of Materials

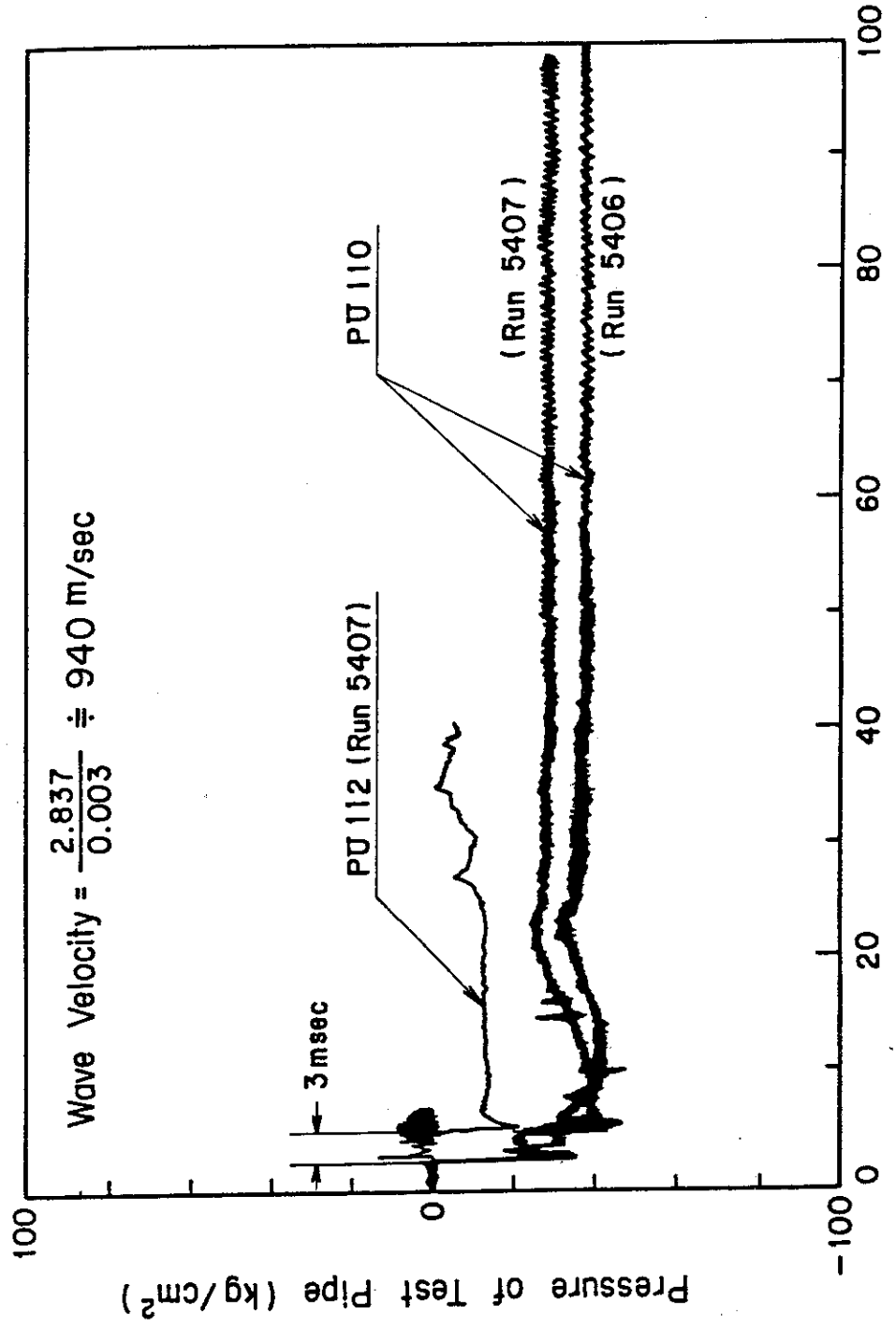

Fig.4.14 Pressure-Time Histories in Test Pipe

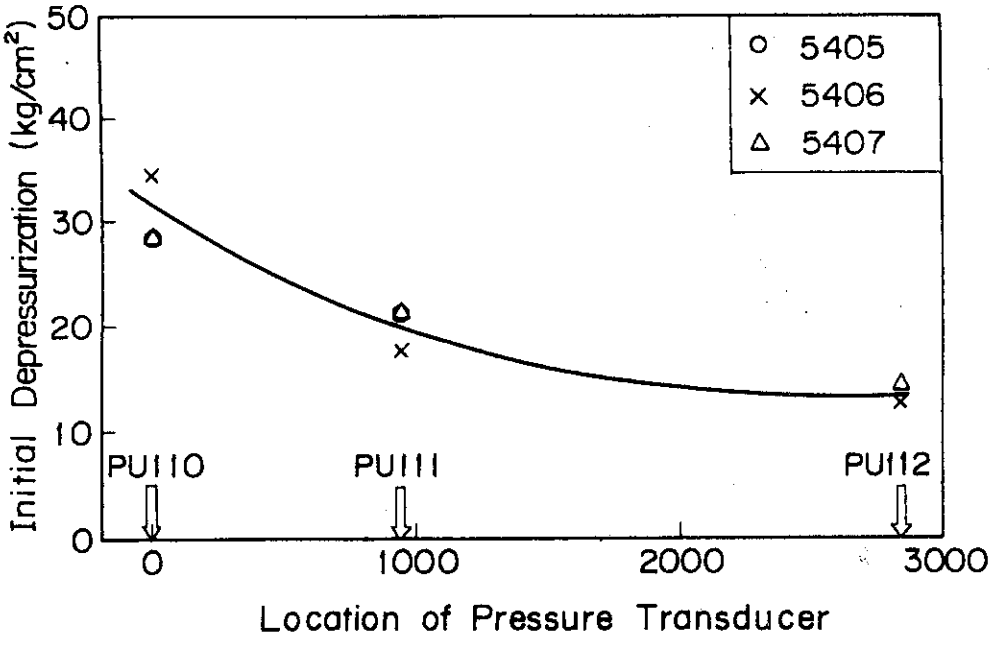

Fig.4.15 Initial Depressurization in Test Pipe

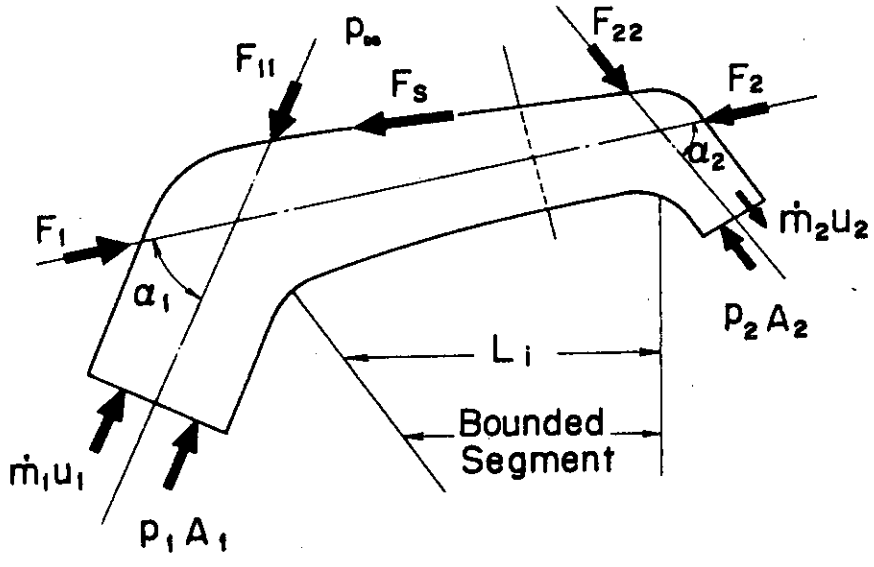

Fig.4.16 Pipe Reaction Forces

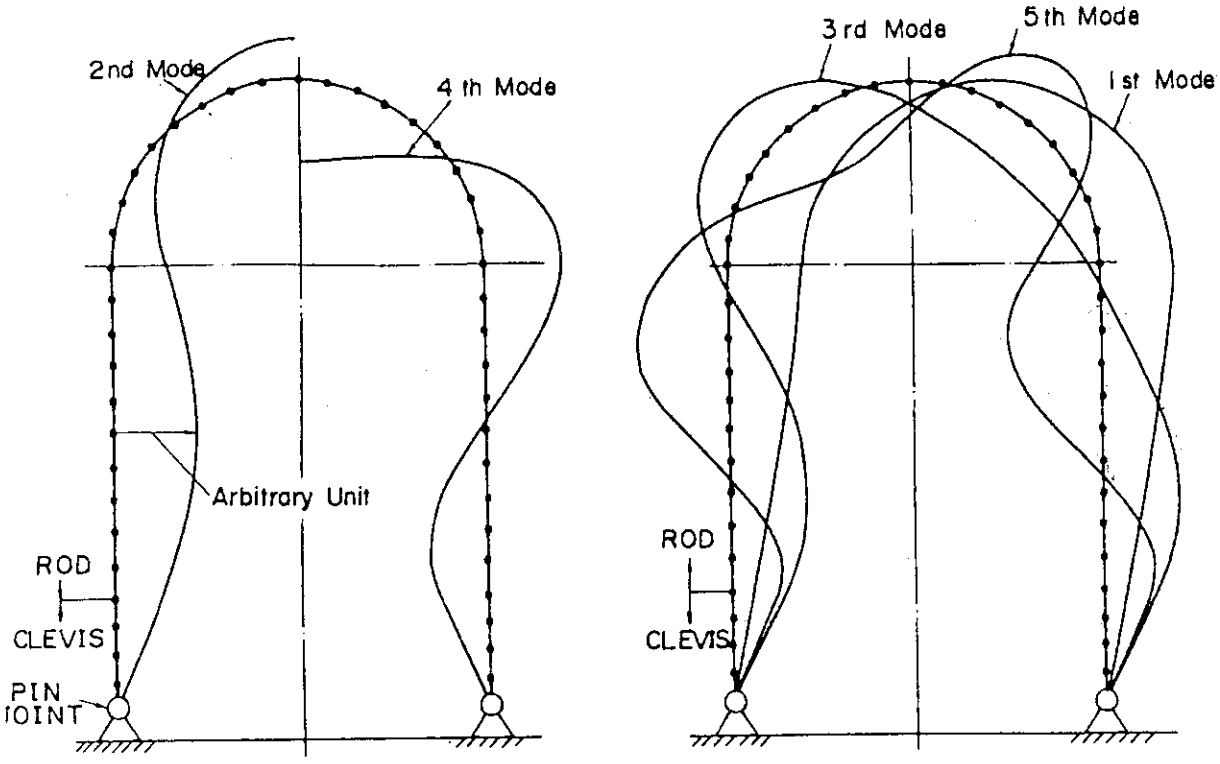

Fig. A1 Shapes of Lowest Five Characteristic Vibration Modes of Restraint

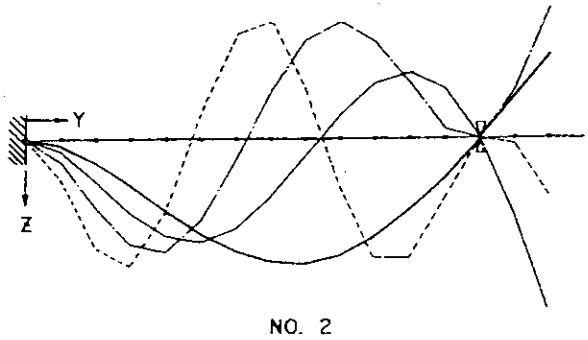

NO. 2

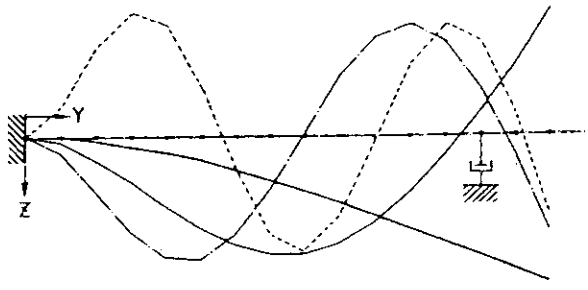

NO. 3

Fig. A2 Shapes of Lowest Four Characteristic Modes of Test Pipe

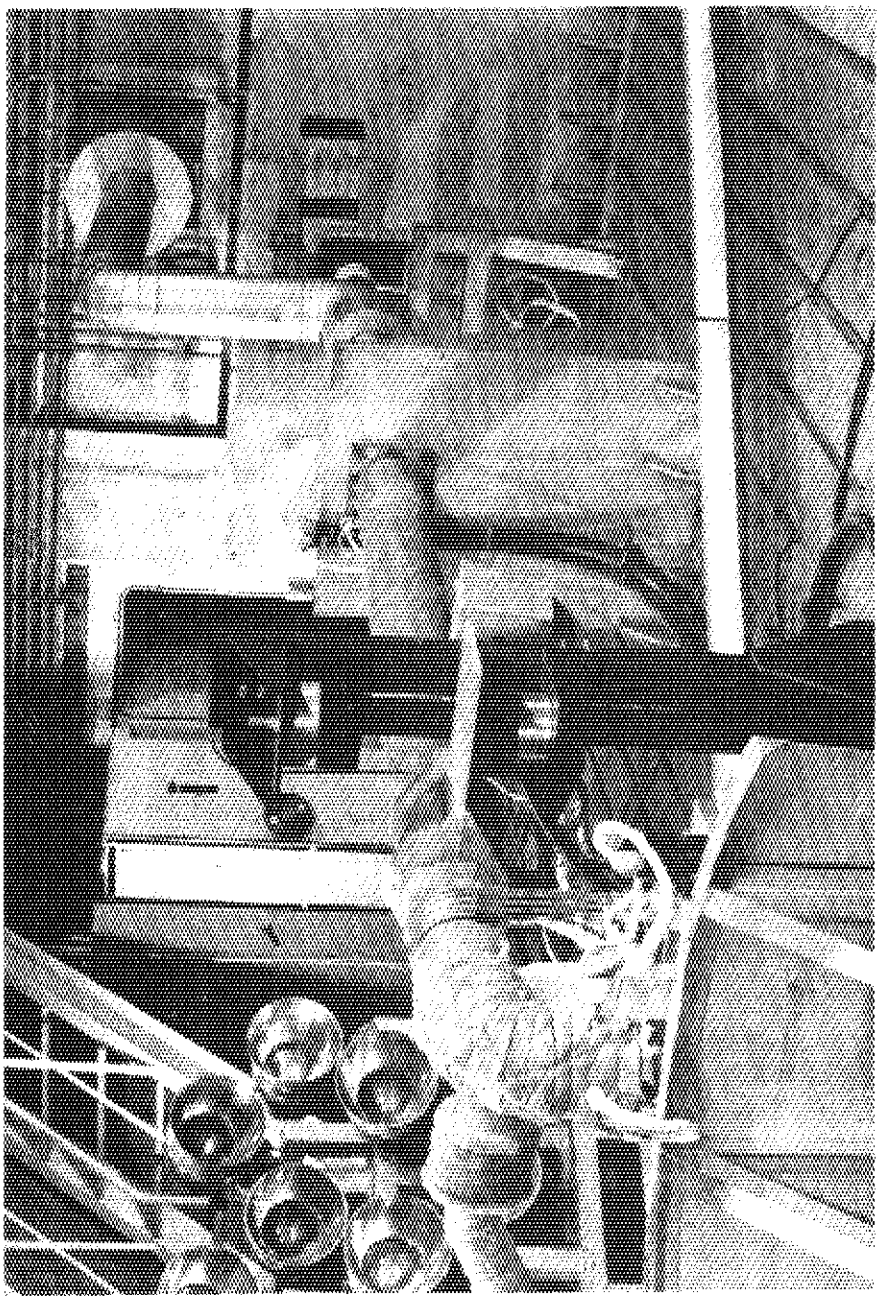

Photo.1 Overall View of Test Section for Pipe Whip (Run 5405)

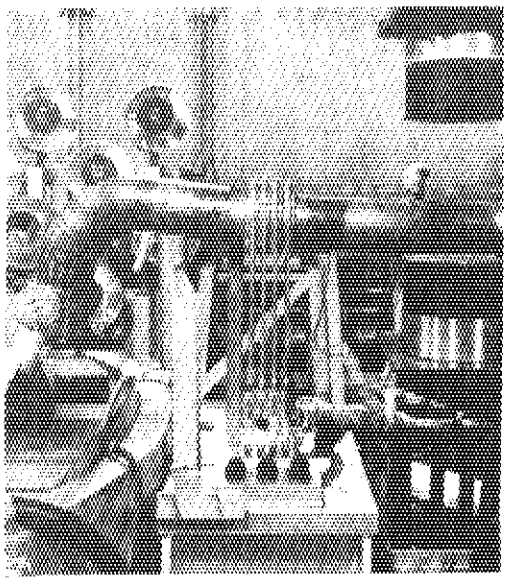

RUN 5405

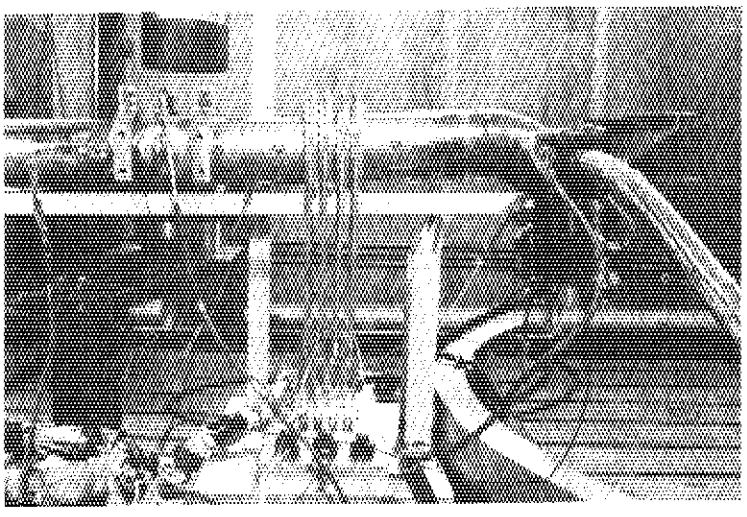

RUN 5406

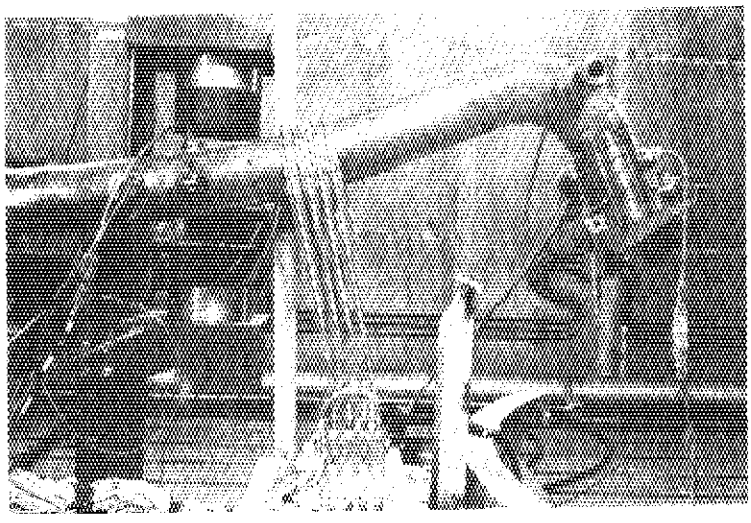

RUN 5407

Photo.2 Deformation of Pipe and Restraints after Tests

	5405		5406		5407
	2.4mS/frame	2mS/frame	1mS/frame	1mS/frame	12.5mS/frame

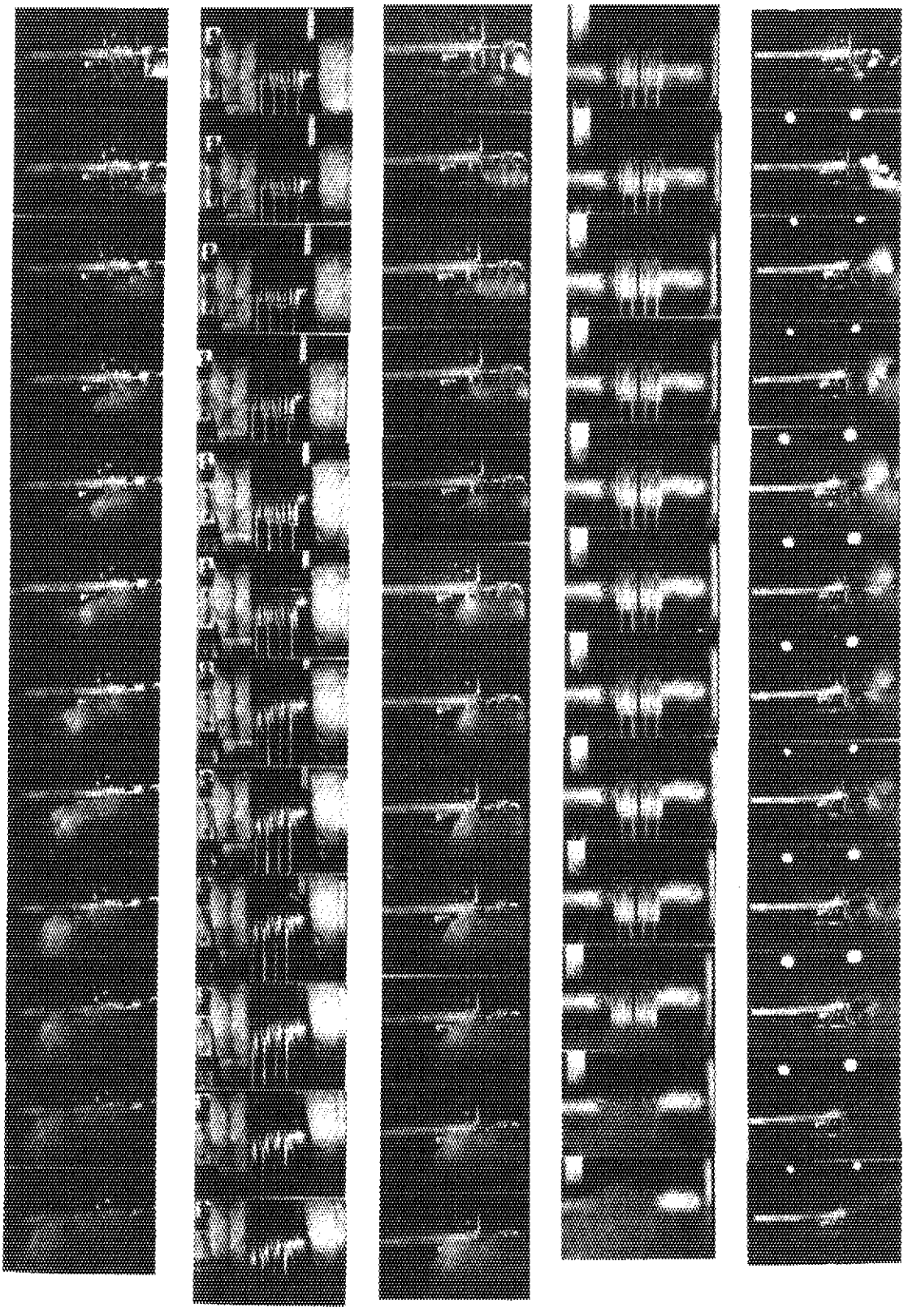

Photo.3 Results of High Speed Camera Photography